Design of Testing Signal for Simulating Nonlinearity of Power Amplifiers

Student: Hsin-Hua Huang **Advisor: Prof. Tzu-Hsien Sang**

Institute of Electronics
Electrical and Computer Engineering College
National Chiao-Tung University

ABSTRACT

RF circuit design has become a tremendously important research area along with the growing popularity and importance of wireless communications. The linearity of RF devices, such as the power amplifier studied in this thesis, plays a significant role in determining the overall system performance. Therefore, evaluating power amplifiers' behavior, whether by measuring or simulating with the design, can provide valuable information for the design process. This thesis reports my research on the modeling and simulation of power amplifiers. First, I studied the modeling issues with the focus on nonlinearity and linear memory. A proper modeling can provide us the

insights of the causes and effects of the non-ideal behaviors of power amplifiers. In practice, the modeling parameters can be extracted by measuring the outputs with selected excitation signals, such as single-tone, two-tone and multi-tone signals. In the second part of this thesis, I try to evaluate the non-ideal effects by simulations instead of physically measuring a circuit. I focus my effort for Orthogonal Frequency-Division Multiplexing (OFDM) systems. In such systems, non-ideal effects are summarized by measuring the Error Vector Magnitude (EVM). It is very time-consuming if the simulation is conducted by inputting pseudo-random OFDM signals and measuring the EVM output. To speed up the simulation time, I developed a specially designed OFDM signal which satisfies certain spectral and statistic properties.. Experiments show that using the designed signal can drastically reduce simulation time and generate comparable EVM values as compared to using pseudo-random OFDM signals.

Index Terms: Power amplifier, Modeling, Nonlinear with Linear Memory, Multi-tone testing, QPSK, OFDM, Gaussian PDF.

用於功率放大之非線性特性之
特殊測試訊號設計

學生: 黃昕華　　指導教授: 桑梓賢教授

國立交通大學

電子工程學系　電子研究所碩士班

摘要

射頻電路設計隨著無線通信的日益增多，成為一個明顯重要的研究課題。射頻元件的特性，例如在這篇論文裡研究的功率放大器，在確認系統性能中，能起重要作用。因此，評估功率放大器的特性，無論是透過測量還是模擬，都能提供對設計過程有價值的訊息，而這篇論文，報告我的對功率放大器的模型化和模擬方法的研究。首先，我集中於非線性和線性記憶的模型化。適當的模型化，能為我們提供功率放大器的非理想特性的洞察力。實際上，模型參數可以被萃取，那靠一些測試訊號信號，例如單音調，雙音調和多重音調的信號。在這篇論文的第二個部分，我透過模擬來取代實際電路的量測，集中研究正交分頻多工系統。在這樣的系統裡，非理想的效應透過錯誤向量振幅的測量。如果用隨機的正交分頻

多工信號作模擬，要錯誤向量振幅的結果將非常費時。為加速模擬時間，我研究一種特別設計正交分頻多工信號。實驗顯示，使用被設計的信號能大量降低模擬時間，並且與使用隨機正交分頻多工信號相比，可產生粗略的錯誤向量振幅值。

ACKNOWLEDGMENTS

首先感謝我的指導教授桑梓賢博士，之前遭遇到相當大的瓶頸，茫然困窘而不知何去何從，非常感謝桑老師幫我打開另一扇窗，讓我又見到希望的光芒。雖然相處只有短短一年，不過桑老師總是像火車頭一樣引領我，令我獲益匪淺得到許多地指導，學生將謹記在心中。

再來感謝相處兩年的室友香蕉、北鴨、和凱吉，還有朋友塔哥、師兄、助理……，常常為我打氣。當初談天說地的情景，會是以後讓我懷念不已的回憶。另外還要感謝學長台佑、豪哥……，學弟阿天、阿祥、昕爺、Kitty……，還有來不及熟稔的阿賢、俊育……，當初協助我解決不少問題和麻煩，感謝你們熱心地幫忙，讓我能有更多心力集中在課業上。要感謝的人很多，這邊就沒辦法一一舉出了，但是謝謝你們的援手，將我一步步推向終點。

最後，我要感謝我的家人和女友燕，一直給予信心和勇氣，你們是我奮鬥的動力。很抱歉讓父母您們多操勞這些年，我會接下責任和重擔，您們可以安心頤養天年了。還有女友燕，默默地鼓勵和支持，謝謝你們。

Figure Captions

Chapter 1
Introduction

1.1 MOTIVATION

In this thesis, I studied the non-ideal behavior of RF (Radio Frequency) components in communication systems. Generally speaking, wireless transmitters and receivers can be separated into the baseband and RF sections. The bandwidth of the baseband section determines the rate that data can flow through the system. The design of the baseband aims at improving the fidelity of the data stream being communicated. The RF section of the transmitter converts the baseband signal up to the assigned channel and injecting the signal into the medium. Conversely, the RF section of the receiver takes the signal from the medium and converts it back down to baseband frequency. The RF systems are constructed primarily by four building blocks — amplifiers, filters, mixers, and oscillators. The power amplifier (PA) is an important part in the RF system. The power amplifier provides the energy to transmit the signal from antenna to receiver. However, the power amplifier costs a lot of energy in all wireless system and had a lot of area in RF circuit. The design of the power amplifiers attracts a lot of attention in both practice and research..

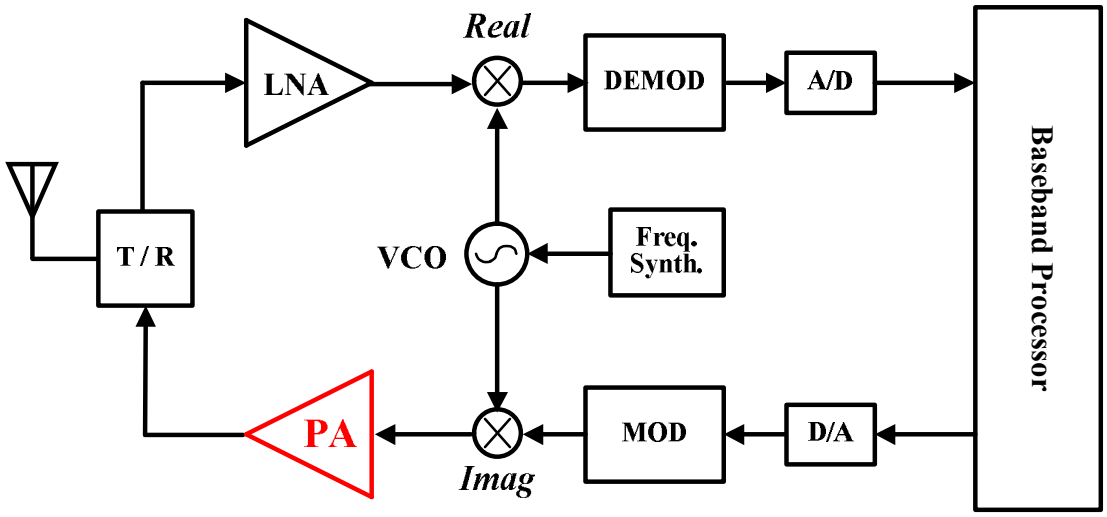

Figure 1 - 1 The typical wireless system.

In the process of designing a suitable power amplifier, it is often to set up a model for simulations [1]. By modeling, the system could simulate very easy and fast and could find out the problems coarsely. The important characteristics of the power amplifier are power efficiency and linearity. This thesis reports a research on power amplifiers that would usually suffer from the nonlinearity of the transistors. In order to measure the parameters of the model, testing signal should be designed at first. The regular testing signals of the power amplifier are single-tone, two-tone, and the Orthogonal Frequency Division Modulation (OFDM) signal. The pseuro-random OFDM testing signal usually need a lot of time to simulate. If the engineers could design a special OFDM signal that has the certain special properties of the pseudo-random OFDM signals, then, the simulation time would reduce a lot.

1.2 THESIS ORGANIZATION

This chapter, Chapter 1, includes the some background knowledge of the wireless system, motivation and the thesis organization of this thesis.

Chapter 2 introduces some background knowledge of power amplifiers and several model types of the nonlinear power amplifiers.

In Chapter 3, this thesis introduces the measurement process with various input signals, and how to design an OFDM signal with a specified Probability Density Function (PDF) envelope.

The last chapter, Chapter 4, recapitulates the major considerations of this thesis and concludes with suggestions for future investigation.

Chapter 2
Models of Power Amplifier

2.1 Overview of Power Amplifier

The RF power amplifier is an electrical device to convert the signals into the larger signals [2]. The two types of RF power amplifiers are traveling-wave tube amplifiers (TWTAs) and solid-state power amplifiers (SSPAs). The SSPAs are typically used at the lower frequency bands, and the basic building block of the SSPA is composed of the power transistors. The main characteristics of an amplifier are linearity and efficiency. The definition of the efficiency can be represented in the form as

$$\eta_c = \frac{RF\ output\ power\ P_o}{DC\ input\ power\ P_{DC}}, \tag{2.1}$$

where the amplifier could be figured out by the value of the parameter η_c.

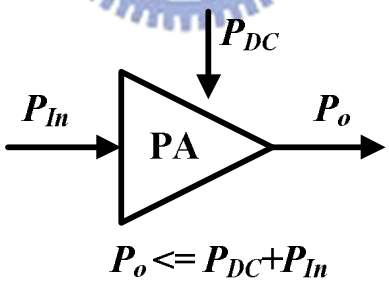

Figure 2 - 1 Power amplifier.

In general, the power amplifiers are classified according to their circuit configurations and methods of the operations. The class of operation has very important implications for power amplifiers in terms of linearity and efficiency. They are intended for two types, linear operation (Class A, B, AB and C) or constant-envelope operation (Class D, E and F). The following is brief description of some of the more common amplifier classes. This paper is focus on the linear

operation type power amplifiers. Then, the constant-envelope operation power amplifiers will be introduced by a short section. The common linear power amplifier is shown in Figure 2-2 and 2-3.

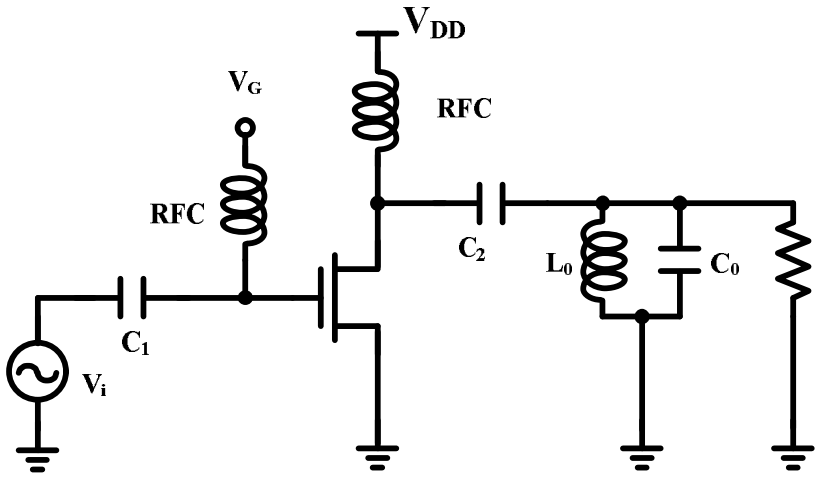

Figure 2 - 2 Single-ended power amplifier (Class A, B or C).

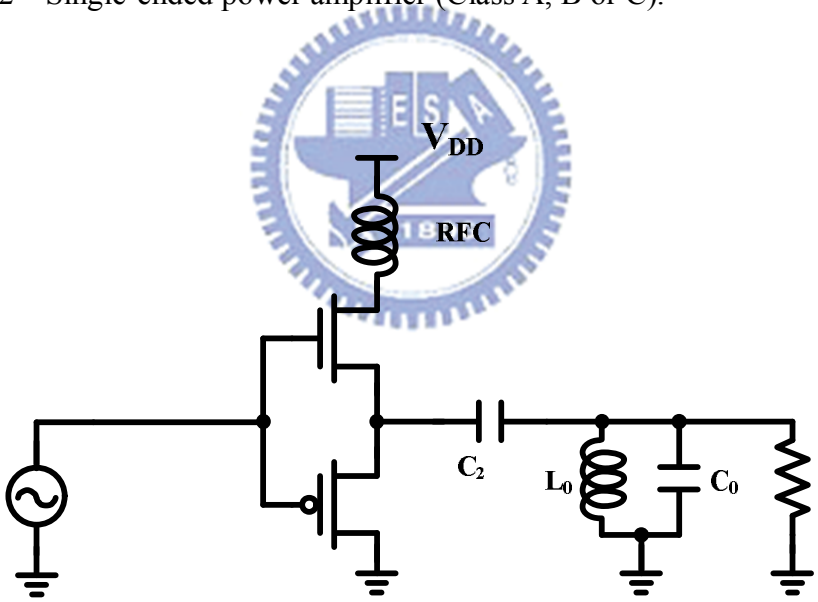

Figure 2 - 3 Complementary push-pull power amplifier (Class A, B or C).

2.1.1 CLASS A

Class A amplifiers have the highest linearity so they have very low distortion. However, they are very inefficient so they are rarely used for high power designs. Because output devices conducted through 360 degrees of input cycle (never switch off), a lot of power was dissipated in the devices. The efficiency of the class A is

shown in followings. The maximum of Class A efficiency is about 50%.

$$P_{DC} = \frac{V_{DD}^2}{R_L} \tag{2.2}$$

$$P_L \approx \frac{V_O^2}{2R_L} \tag{2.3}$$

$$\eta_{ClassA} = \frac{P_L}{P_{DC}} \approx \frac{V_O^2 / 2R_L}{V_{DD}^2 / R_L} \approx \frac{V_O^2}{2V_{DD}^2} \leq 50\% \tag{2.4}$$

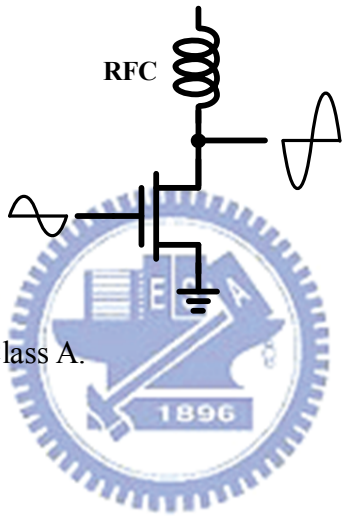

Figure 2 - 4 Waveform of Class A.

2.1.2 CLASS B

Class B amplifiers are significantly more efficient than class A amplifiers. However, they would have bad distortion when the signal level is low. Output devices conducted for 180 degrees (1/2 of input cycle), and this distortion of operation is also called crossover distortion. Then, the class B power amplifiers are usually used the push pull structure to make a sine-wave. The efficiency of the class B is shown in followings. The maximum of Class B is about 78%.

$$P_{DC} = \frac{2 \cdot V_{DD} \cdot V_O}{\pi \cdot R_L} \tag{2.5}$$

$$P_L \approx \frac{V_O^2}{2R_L} \tag{2.6}$$

$$\eta_{ClassB} = \frac{P_L}{P_{DC}} \approx \frac{V_O^2 / 2R_L}{2 \cdot V_{DD} \cdot V_O / \pi \cdot R_L} \approx \frac{\pi \cdot V_O}{4 \cdot V_{DD}} \leq 78\% \qquad (2.7)$$

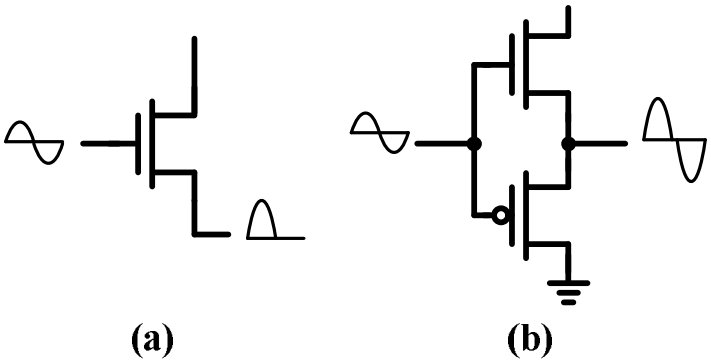

Figure 2 - 5 (a) Waveform of single-ended Class B (b) Push-pull Class B.

2.1.3 CLASS AB

Class AB is probably the most common amplifier because it combines the advantages of class A and B amplifiers. The current signal between class A, class B and class AB could be shown in Figure 2-6. They have the improved efficiency of class B amps and distortion performance that is a lot closer to that of a class A. The Class AB amplifiers would use pairs of transistors, both of them being biased slightly on so that the crossover distortion is largely eliminated.

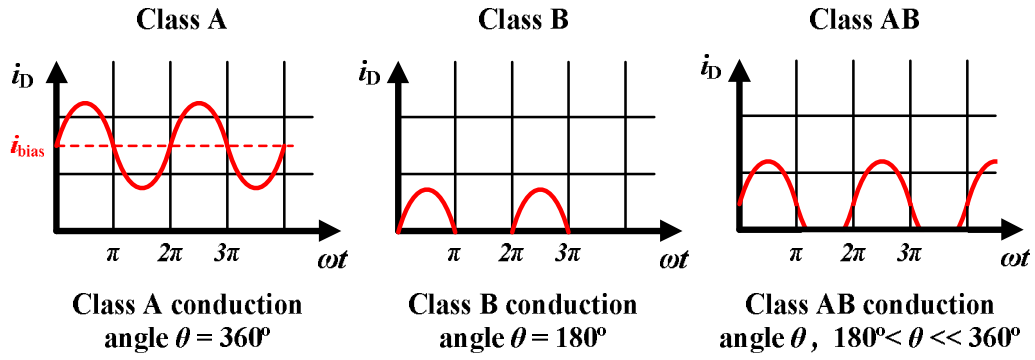

Figure 2 - 6 Waveform of drain's current.

2.1.4 OTHER CLASSES

The previous classes, A, B, and AB are considered linear amplifier, where the

output signal's amplitude and phase are linearly related to the input signal's amplitude and phase. In the application where linearity is not an issue, and efficiency is critical, nonlinear amplifier classes (C, D, E, or F) are used. The transistors of the nonlinear power amplifiers are the switches and only works on the saturation and cutoff regions. As a result, these types of the power amplifier are not the focuses of this paper.

2.2 MODELS OF POWER AMPLIFIER

Power amplifier is an important block in RF system. Through power amplifier models, we could understand their behavior and optimize their performance. According to data type, power amplifier models could be divided into physical models and empirical models.

Physical models describe their behavior by electronic elements, voltages and currents. They also provide high accuracy by many parameters. Unfortunately, we have more parameters, and we spend more simulation time. Moreover, if we would like to get these parameters, we need to a lot of circuit details and knowledge. So, physical model is unsuitable for system-level analysis.

Empirical models described their behavior by mathematics. Several equations or data tables can describe the power amplifier model, and can be generalized from some tests. If higher accuracy is needed, more tests are needed.

2.2.1 NONLINEAR AND MEMORYLESS MODEL

Memoryless nonlinear models are the simplest. By ignoring the memory effect, behavioral model can focus on envelope transfer characteristics. A general input narrowband input signal $x(t)$ can be described as

$$x(t) = r(t)\cos\left[2\pi f_0 t + \theta(t)\right], \tag{2.8}$$

where $r(t)$ is envelope amplitude and $\theta(t)$ is phase components. The PA output, $y(t)$, as yielded by Equation (2.8), will be represented as

$$y(t) = R(r(t), f_0)\cos\left[2\pi f_0 t + \theta(t) + \Phi(r(t), f_0)\right], \tag{2.9}$$

where nonlinear envelope transfer functions are $R(r(t), f_0)$ and $\Phi(r(t), f_0)$. Equation (2.9) around f_0 is further simplified as

$$y(t) = R(r)\cos\left[\omega_0 t + \theta + \Phi(r)\right], \tag{2.10}$$

where $\omega_0 = 2\pi f_0$. The function $R(r)$ and $\Phi(r)$ represent the nonlinear amplitude-to-amplitude (AM-AM) conversion and nonlinear amplitude-to-phase (AM-PM) conversion. Equation (2.10) could be written in different forms as follow:

$$\begin{aligned} y(t) &= R(r)\cos\left[\omega_0 t + \theta + \Phi(r)\right] \\ &= R(r)\cos\Phi(r)\cos\left(\omega_0 t + \theta\right) - R(r)\sin\Phi(r)\sin\left(\omega_0 t + \theta\right) \\ &= In(r)\cos\left(\omega_0 t + \theta\right) - Qu(r)\sin\left(\omega_0 t + \theta\right), \end{aligned} \tag{2.11}$$

where in-phase terms, $In(r)$, and quadrature terms, $Qu(r)$, and nonlinearity forms are

$$\begin{aligned} In(r) &= R(r)\cos\Phi(r), \\ Qu(r) &= R(r)\sin\Phi(r). \end{aligned} \tag{2.12}$$

A simple schematic implementation of the quadrature form is shown in Figure 2-7.

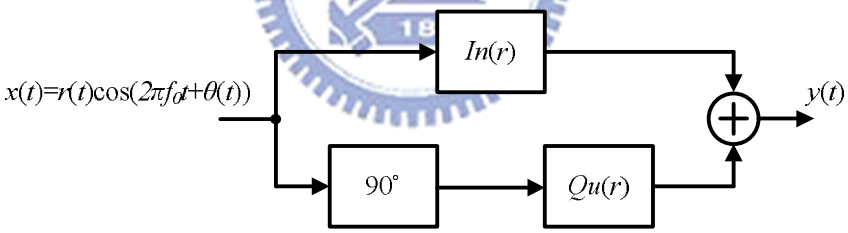

Figure 2 - 7 Quadrature model of a power amplifier.

2.2.2 MODEL TYPE

A. COMPLEX POWER SERIES MODELS

A general form of complex power series model is expressed as

$$y(t) = \sum_{l=1}^{L} k_l x^l(t), \tag{2.13}$$

where k_l are complex coefficients for a lth-order term. The complex power series models need over three terms to achieve sufficient accuracy. However, harmonic and

IMP analysis effects are difficult to separate out from higher-order coefficients.

B. SALEH MODELS

Saleh model [3] defined two parameters in one equation to describe the model characteristics. This model contained two types, polar models and quadrature models. Saleh polar models are written as

$$R(r) = \frac{\alpha_a r}{1+\beta_a r^2}, \tag{2.14}$$

$$\Phi(r) = \frac{\alpha_\theta r^2}{1+\beta_\theta r^2}, \tag{2.15}$$

where α_a, β_a, α_θ and β_θ could be extracted by using the least-squares approximation. Quadrature models could be derived from Saleh polar models. These models could be written as

$$In(r) = \frac{\alpha_I r}{1+\beta_I r^2}, \tag{2.16}$$

$$Qu(r) = \frac{\alpha_Q r3}{\left(1+\beta_Q r^2\right)^2}, \tag{2.17}$$

where the quadrature-model coefficients α_I, β_I, α_Q and β_Q would be extracted independently of the polar-model coefficients α_a, β_a, α_θ and β_θ. However, Saleh model is difficult to process multi-carrier or complex modulated signals because the parameters are too simple. Modified Saleh models are solutions for this problem.

C. MODIFIED SALEH MODELS

A general form of modified Saleh model [3] is written as

$$z(r) = \frac{\alpha r^{\eta}}{\left(1+\beta r^{\gamma}\right)^{\nu}} - \varepsilon, \tag{2.18}$$

where γ is an exponent and ε is a phase shift. The AM-AM $R(r)$ and the AM-PM $\Phi(r)$ are the same form of the equations. In AM-PM conversion, the parameter η is usually equal to zero. The parameters (α, β) could be calculated with different variables (ν, γ). In AM-AM conversion, the parameter η is often equal to one and ε is equal to zero. Moreover, the coefficients (α, β) could be found in the same method.

D. BESSEL-FOURIER MODELS

The Bessel-Fourier model [4] is improved from the memoryless complex Fourier series expansion. The Bessel-Fourier could process not only large and small signals but also simple and complex multi-carrier signals. It is a decomposable model, and separates from zonal-band and harmonic-band. It could be written generally as

$$y(t) = \sum_{k=-\infty}^{\infty} c_k e^{j\alpha k \sum x(t)}, \tag{2.19}$$

and α is defined by the dynamic range. The value of the variable α is an important coefficient. The parameter α is more adequate, and the result is better.

E. HETRAKUL AND TAYLOR MODEL

Hetrakul and Taylor [5] made this quadrature model for TWTA power amplifiers. The model equations could be expressed as

$$\begin{aligned} In(r) &= \alpha_I r e^{-\beta_I r^2} I_0(\beta_I r^2), \\ Qu(r) &= \alpha_Q r e^{-\beta_Q r^2} I_0(\beta_Q r^2), \end{aligned} \tag{2.20}$$

and $I_0(.)$ is the modified Bessel function of the first kind. The extraction of the coefficients α_I, β_I, α_Q, and β_Q required optimization algorithms. In fact, Hetrakul and Taylor model had good approximation of the in-phase equation $In(r)$, but had wrong

approximation of the quadrature equation $Qu(r)$.

F. BERMAN AND MAHLE MODEL

Berman and Mahle [6] made the model and focused on the nonlinear AM-PM characteristics $\Phi(r)$. The $\Phi(r)$ depended on three parameters (α, η, γ):

$$\Phi(r) = \alpha(1 - e^{-\beta r}) + \gamma r. \tag{2.21}$$

The Berman and Mahle model could be combined with others of the AM-AM model.

2.3 NONLINEAR MODEL WITH LINEAR MEMORY

Memoryless nonlinear model assumed that characteristics of the power amplifiers are frequency independent. The model didn't consider memory effect because of narrowband input signals. However, the wideband signals are generally used in modern communication systems. Modeling PAs with memory and nonlinearity becomes important in wideband system design. This section will focus on linear memory. By using linear filter, the model can be analyzed in frequency domain.

2.3.1 TWO-BOX MODELS

The two-box model assumes that memory effects and nonlinearity are independent of each other. The model has two subsystems to separate out frequency equations and envelope equations. The two-box model would be expressed as two types: the Wiener model (memory-nonlinear) and the Hammerstein model (memory-nonlinear) in Figures 2-8 and 2-9.

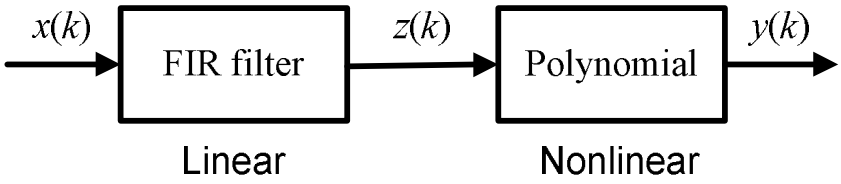

Figure 2 - 8 The Wiener model.

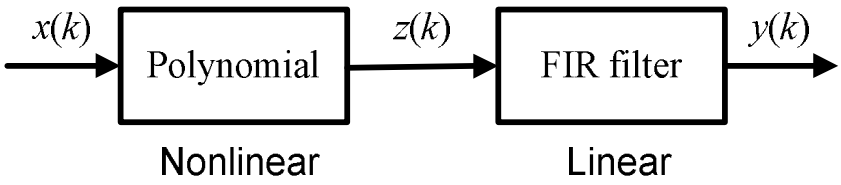

Figure 2 - 9 The Hammerstein model.

The equations of linear filter are shown below. The filter in the Wiener model is

$$y_{W,F}(k) = \sum_{q=0}^{Q-1} h(k)x(k-q), \tag{2.22}$$

and the filter in the Hammerstein model is given by

$$y_{H,F}(k) = \sum_{q=0}^{Q-1} h(k)z(k-q). \tag{2.23}$$

The nonlinearity block is composed by a power series, and the block in the Wiener model is

$$Y_{W,NL}(s) = \sum_{n=0}^{N} c^{(n)} Z^n(s), \tag{2.24}$$

and the block in the Hammerstein model is represented as

$$Y_{H,NL}(s) = \sum_{n=0}^{N} c^{(n)} X^n(s). \tag{2.25}$$

However, the parameters of two-box have to be estimated from swept-tone signals. More details about swept-tone or multi-carrier measurements will be introduced in Chapter 3. The power amplifier is a holistic circuit so it is not straightforward to

separate the memory effect from nonlinearity. Many engineers have tried their hands on this task. In the following, some methods will be presented in sketch.

2.3.2 FILTER AND NONLINEAR BLOCK ESTIMATION

A. FREQUENCY DOMAIN ESTIMATION

The method estimates frequency response by using the input and output power spectrum. With mathematics, it could be explained by

$$S_{xy}(f) = \int_{-\infty}^{\infty} R_{xy}(\tau) \cdot e^{-j2\pi f\tau} d\tau. \tag{2.26}$$

$R_{xy}(\tau)$ is cross-correlation function, and $S_{xy}(f)$ is Fourier transform pair of $R_{xy}(\tau)$. The transfer function of the filter could be estimated as

$$S_{xx}(f) = \int_{-\infty}^{\infty} R_{xx}(\tau) \cdot e^{-j2\pi f\tau} d\tau. \tag{2.27}$$

$$\hat{H}(f) = \frac{S_{xy}(f)}{S_{xx}(f)}. \tag{2.28}$$

However, this estimation method might need enough averaging to decrease the random error.

B. LEAST-SQUARES METHOD

The least-squares method [7] estimates the filter by using matrix vector. The matrix X for K measurements is expressed as

$$X = \begin{bmatrix} x(Q) & x(Q-1) & \cdots & x(1) \\ x(Q+1) & x(Q) & \cdots & x(2) \\ \vdots & \vdots & \ddots & \vdots \\ x(Q+K-1) & x(Q+K-2) & \cdots & x(K) \end{bmatrix}_{K\times Q} \tag{2.29}$$

Then parameter vector $\hat{O}$ is defined as

$$\hat{O} = \begin{bmatrix} \hat{h}(0) \\ \hat{h}(1) \\ \vdots \\ \hat{h}(Q-1) \end{bmatrix}_{Q\times 1} . \tag{2.30}$$

$$\hat{O} = (X^H X)^{-1} X^H y. \tag{2.31}$$

The variable X^H is a Hermitian matrix of the matrix X. This expression is also known as the Wiener filter.

C. NONLINEAR BLOCK ESTIMATION

The nonlinear block of the two-box model could be calculated by using least-squares method. On the other hand, there are two kinds of estimation specially using orthogonal polynomial, Chebyshev polynomials and Hermite polynomials. These polynomials would be the best model for some special input signals [reference?].

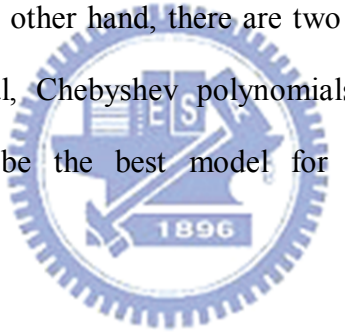

2.3.3 THREE-BOX MODELS

The three-box model improves from the two-box model and it is built by combining the Wiener model and the Hammerstein model by an addition filter. Therefore, the three-box model is also called as the Wiener-Hammerstein model and shown in Figure 2-10.

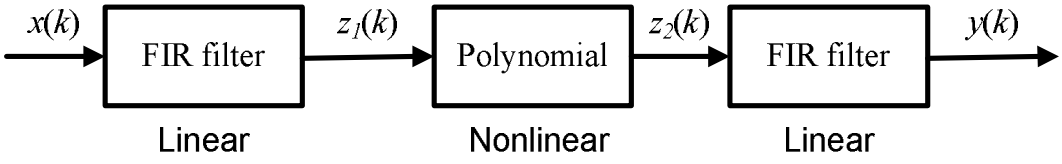

Figure 2 - 10 Three-box model structure.

Now, the structure had two linear filters and one nonlinear block. Chapter 3 will show how to separate out the function of each block. This section will present shortly several kinds of three-box model.

A. INSTANTANEOUS QUADRATURE MODEL

The implementation was presented by Loyka and the structure was presented in Figure 2-11 and 2-12.

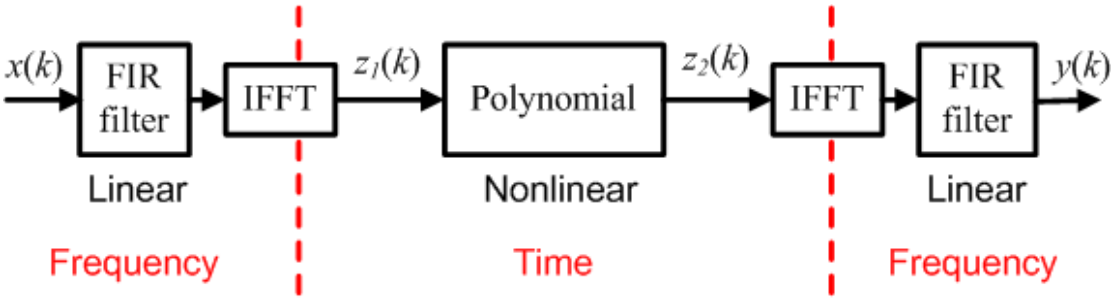

Figure 2 - 11 Instantaneous quadrature technique.

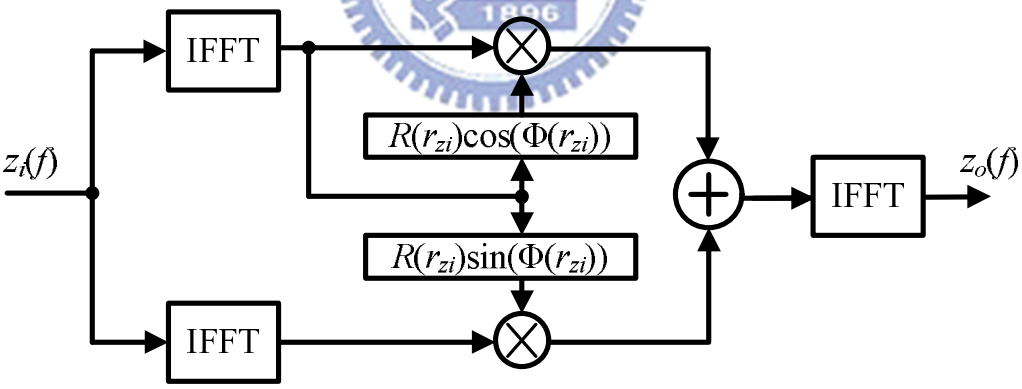

Figure 2 - 12 Implementation of the static nonlinearity of the instantaneous quadrature technique.

The first and third of the blocks process frequency-domain signal representations, and the second block processes time-domain signal representations. Therefore, this model needs to have extra transform functions betweeneach block. The output signal in time domain is written as

$$z_o(k) = z_{i,I}(k)R(r_{z_i}(k))\cos[\Phi(r_{z_i}(k))] - z_{i,Q}(k)R(r_{z_i}(k))\sin[\Phi(r_{z_i}(k))], \quad (2.32)$$

where the variables $z_{i,I}(k)$ and $z_{i,Q}(k)$ stand for the Hilbert transform of the in-phase and quadrature elements. The functions $R(.)$ and $\Phi(.)$ are the instantaneous AM-AM and AM-PM conversions [8].

B. POZA-SARKOZY-BERGER MODEL

The Poza-Sarkozy-Berger (PSB) model [7, 9] tries to extend the memoryless model to take account of frequency-dependent behavior. The basic assumption of the PSB model is that input and output power spectrum would have the same shape. Then, all conversions could be calculated by shifting a reference conversion. This idea is expressed in Figure 2-13 and 2-14.

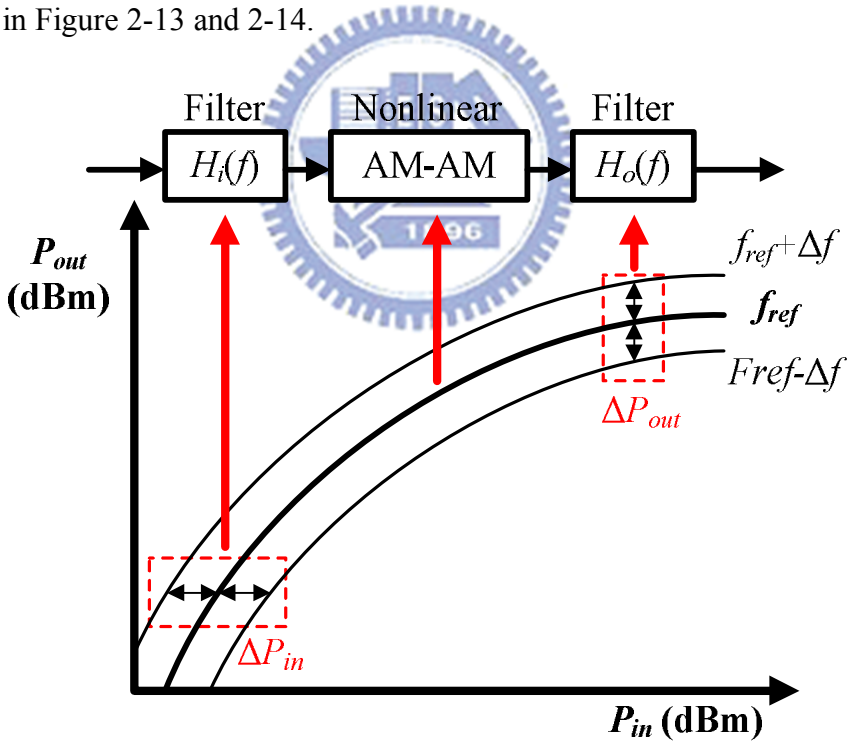

Figure 2 - 13 The AM-AM portion of the PSB model.

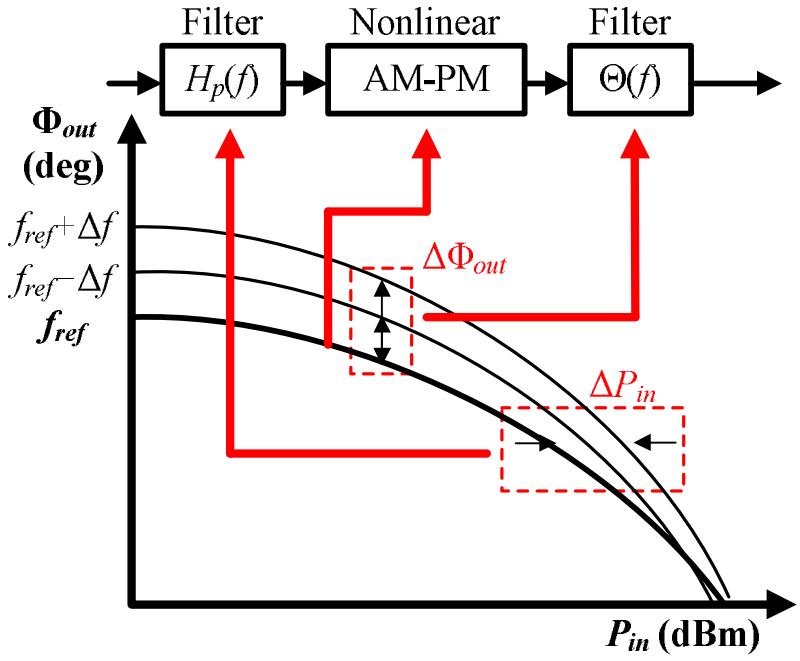

Figure 2 - 14 The AM-PC portion of the PSB model.

The several single-tone measured signals are recorded in the diagram. The AM-AM conversion trace is shifted along the horizontal axis by the filter $|H_i(f)|$ and along the vertical axis by the filter $|H_o(f)|$. The AM-PM conversion trace is shifted along the horizontal axis by the filter $\Theta(f)$ and along the vertical axis by the filter $|H_p(f)|$. The structure of the PSB model is presented in Figure 2-15 [10].

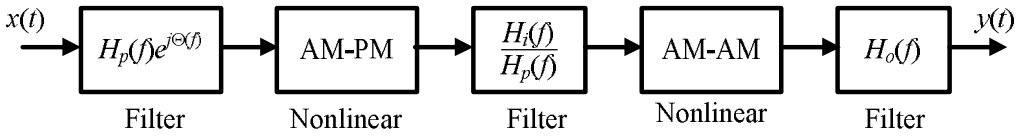

Figure 2 - 15 The complete structure of the PSB model.

At first, a reference frequency f_0 is selected and its AM-AM $R(r, f_0)$ and AM-PM $\Phi(r, f_0)$ performances are measured. In the PSB model, the conversions are $R(r, f_0, \Delta f)$ and $\Phi(r, f_0, \Delta f)$ where the variable Δf is the frequency difference to the reference frequency f_0. Therefore, the characteristics of the power amplifier can be evaluated from the power spectrum measurement of the input and output signal.

C. FREQUENCY –DEPENDENT SALEH MODEL

In previous section, the Saleh model [3] is one kind of the memoryless models. From Equation 2.9 and 2.10, the coefficients α, β are changed into the function $\alpha(f)$ and $\beta(f)$. Here, the functions that are dependent on the frequency could be written as

$$In(r,f)=\frac{\alpha_I(f)r}{1+\beta_I(f)r^2}, \tag{2.33}$$

$$Qu(r,f)=\frac{\alpha_Q(f)r^3}{\left(1+\beta_Q(f)r^2\right)^2}. \tag{2.34}$$

The implements are shown in Figure 2-16.

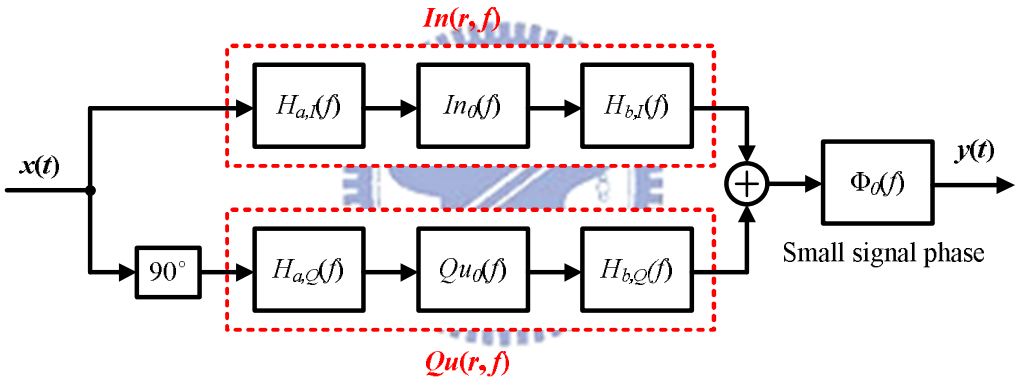

Figure 2 - 16 Frequency-dependent Saleh model.

The function $\alpha(f)$ and $\beta(f)$ could construct the filter in the Figure 2-16. The additional filter $\Phi_0(f)$ is called small-signal phase and is measure for $r\rightarrow 0$. Moreover, the Equation (2.33) and (2.34) could be rewritten in the modified Saleh model. Then, the AM-AM and AM-PM characteristics would be more improved.

$$H_{a,I}(f)=\sqrt{\beta_I(f)}, \tag{2.35}$$

$$H_{a,Q}(f)=\sqrt{\beta_Q(f)}, \tag{2.36}$$

$$H_{b,I}(f) = \alpha_I(f) \Big/ \sqrt{\beta_I(f)}, \tag{2.37}$$

$$H_{b,Q}(f) = \alpha_Q(f) \Big/ \sqrt{\beta_Q(f)}. \tag{2.38}$$

2.3.4 PARALLEL-CASCADE MODELS

This section is an introduction of the poly-spectral models including linear memory and the Abuelma'atti model. The Abuelma'atti model used the first-order Bessel function series $J_1(kr)$ to implement nonlinearities. Then, the Abuelma'atti model consists of a frequency-independent quadrature model that could be combined with the linear memory filter. The equations would be expressed as

$$In(r,f) = \sum_{m=1}^{M} H_{In,m}(f) J_1(\alpha m r), \tag{2.39}$$

$$Qu(r,f) = \sum_{m=1}^{M} H_{Qu,m}(f) J_1(\alpha m r), \tag{2.40}$$

where $H_{In,m}(f)$ and $H_{Qu,m}(f)$ are the frequency-dependent filters. The structure is shown in Figure 2-17.

This model, like as the Bessel-Fourier model, could be fitted by using a least-squares method. The Abuelma'atti models have the perfect characteristics of the in-phase channel. However, in the quadrature channel, when power is over 12dBm, the representation error is decreasing. In higher power system, the Abuelma'atti model is still greater than the frequency-dependent Saleh model.

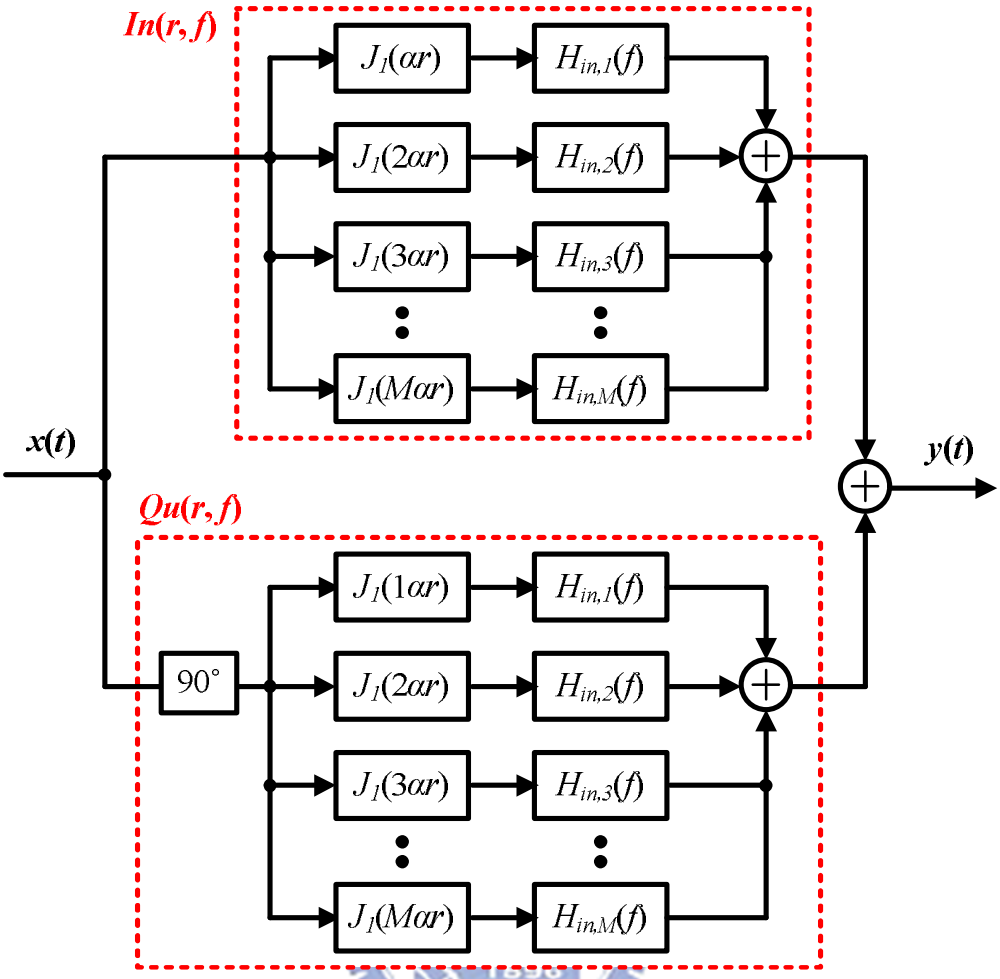

Figure 2 - 17 Abuelma'atti model structure.

2.4 NONLINEAR MODEL WITH NONLINEAR MEMORY

The AM-AM and AM-PM conversions of the nonlinear memory models will no longer depend on the envelope function $r_x(t)$. Here, the model will be considered as the impulse response $h_z(t)$ of a filter. In mathematics, it could be expressed as

$$\begin{aligned} y(t) &= f(r_x(t), z(t)) r_x(t) e^{j\theta(t)} \\ &\approx f_0(r_x(t))[1 + h_z(t) * r_x(t)] \cdot r_x(t) e^{j\theta(t)}, \end{aligned} \tag{2.41}$$

where $f_0(r_x(t))$ is the AM-AM and AM-PM transfer functions in the memoryless system [12]. The model structure is shown in Figure 2-18.

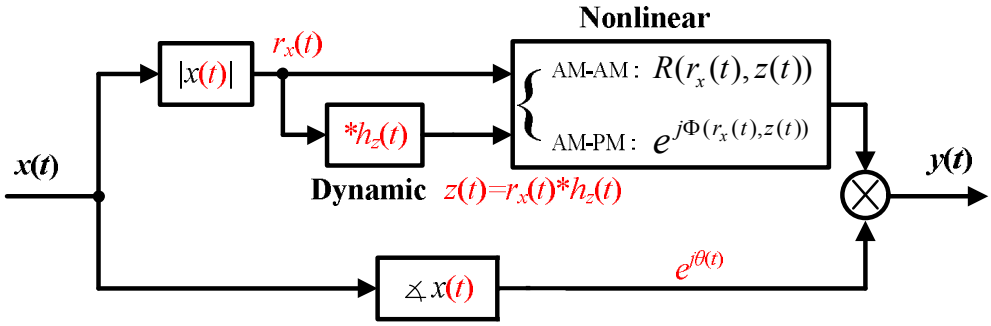

Figure 2 - 18 Nonlinearly dependent on the instantaneous envelope amplitude and a linear dynamic parameter.

The nonlinear model with nonlinear memory can be described by an artificial neural network (ANN) or parallel structure. In a general nonlinear finite impulse response model, it could be approximated by a first-order Taylor series expansion:

$$y(t) \approx \sum_{q=1}^{Q} f_q(x_0(t), \tau_q) x(t-\tau_q), \tag{2.42}$$

where $x_0(t)$ is predetermined nonlinear memoryless operation state. The output signal is relative with a time-variant parameter τ_q. The memory polynomial model is the simplest modeling expression. Then, the parallel Wiener model is well-known, and it could model the nonlinear memory effect adequately by using a linear-time-invariant (LTI) system to process the memoryless part. The Volterra-series-based models are especially suitable for weakly nonlinear system. However, when the system has complex nonlinear characteristics, to compute the Volterra kernels is difficult. Finally, this paper will focus on the nonlinear model with linear memory so it is a short introduction of the model with nonlinear memory.

2.5 SUMMARY

Memoryless nonlinear models have been researched for many years. The complex power series, Saleh, Bessel-Fourier models are more popular in these models.

From these models could be extracted the envelope transfer characteristics of the AM-AM and AM-PM conversions. The complex power series might become a little complex when the power amplifier has strong nonlinearities. The Saleh and modified Saleh models can be used in the computer model because the parameters of the models can be extracted by a least-squares method or a similar optimization process. However, besides the Bessel-Fourier model, decomposing the model for IMP analysis is very difficult. The Bessel-Fourier model might have a better accuracy in the nonlinear models and could handle AM-AM and AM-PM easily.

Linear memory models could be divided easily into the nonlinear static part and frequency-dependent part. The nonlinear part is the same as the previous section. The filter, frequency-dependent part, is assumed that the nonlinear curve will sweep linearly. The popular model is a three-box model, especially the PSB model. Another method is adding some frequency-dependent parameters, like the Saleh model does. Another way is using many parallel paths with the different filters and functions. The Abuelma'atti model structure is a famous model of them.

Finally, this paper will focus on the nonlinear model with linear memory without much concern about the nonlinear memory.

Chapter 3
Multi-Carrier Signal Measurement

3.1 SINGLE-TONE AND TWO-TONE MEASUREMENT

In the power amplifier design, efficiency and linearity is always our focus. However, there is always a trade-off between efficiency and linearity. In the designing process, an early-on simulation based on proper PA models can provide useful information for fine-tuning the design. In Chapter 2, many PA models are introduced. How can we verify whether a given model is adequate? In general, the process in Figure 3-1 can answer this question.

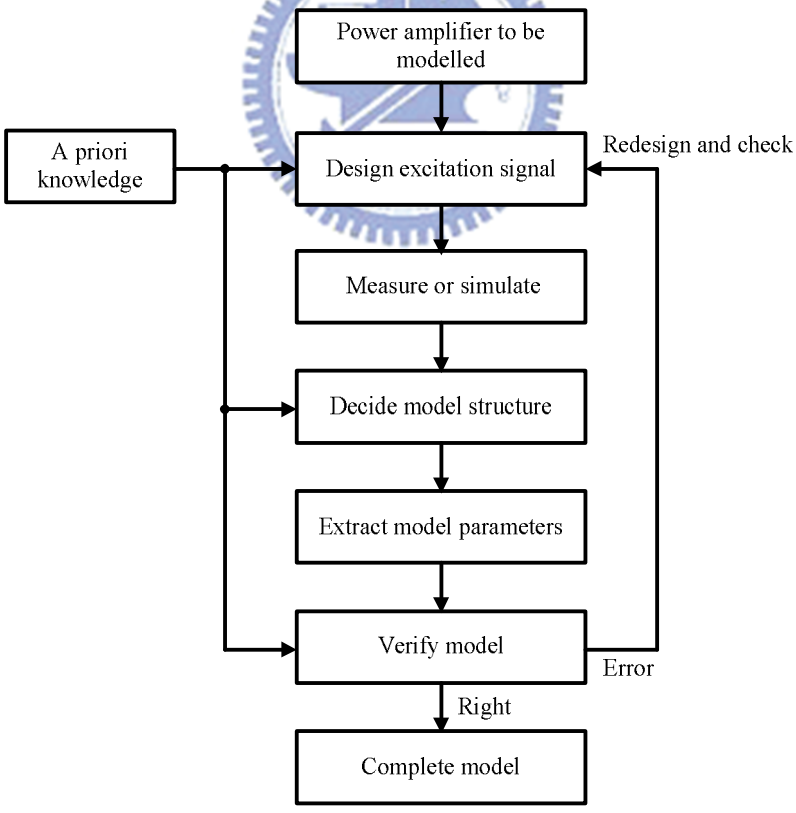

Figure 3 - 1 System model identification [13].

According the information of the amplifier, the excitation signal can be designed

beforehand. The suitable excitation signal could have a significant influence on the characteristics of the model. Then, the measurement is conducted with persistent excitation. Because the power amplifiers are usually designed into the band-limited structure, the sine or multi-sine signals are also usually used to test the device under test (DUT). Some typical signals in system identification, like step function or pseudo-random binary sequences, are unsuitable to test the characteristics of the RF power amplifier because they are low-pass filtered or only modulated on a carrier signal. The more complex or non-periodic signals can make the accuracy of measurement higher, but we hope that the test signals can also make the process easier. Usually, the multi-sine test signal is composed of four carriers at least. The next section hasa short introduction of the testing signals.

3.1.1 POWER AMPLIFIER MEASUREMENT

The measurement of the power amplifier can observe many items, like noise figure, stability, matching, etc. However, the most important trade-off in power amplifier design is between efficiency and linearity. Now, the follow will discuss two properties.

A. EFFICIENCY

Drain efficiency and power added efficiency (PAE) are two measurements of the power amplifier efficiency. Drain efficiency is defined in Equation (2.1) in the section 2.1, and it is a ratio of the output power to the dc consumed power. Power added efficiency (PAE) is a more practical measurement, and the PAE is defined in Equation (3.1). The PAE is a ratio of the difference between the output power and the input power to the dc consumed power.

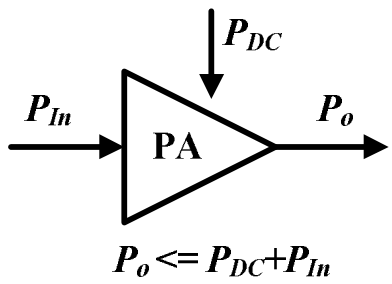

Figure 3 - 2 Power amplifier.

$$\eta_{PAE} = \frac{P_o - P_{In}}{P_{DC}}. \tag{3.1}$$

B. LINEARITY

Power amplifier [2] nonlinearity of the design is usually characterized by IIP_3 and 1 dB compression measurements. Use a two-tone test to measure I_{IP3}. By sweeping the power level of the large tone, measure the 1dB compression point in Figure 3-2, Figure 3-3 and Figure 3-4. The curve has a little nonlinearity around the higher power. The point P_{1dB} is defined when the difference between an ideal linear curve and a real curve is 1 dB. The nth-order inter-modulation distortion is called IMD_n, and 1dB gain compression point is called P_{1dB}. The parameter IP_3 is defined as the 3rd-order intercepts point. The input power of the point IP3 is defined as IIP_3, and output power is defined as OIP_3 and shown in the Figure 3-5.

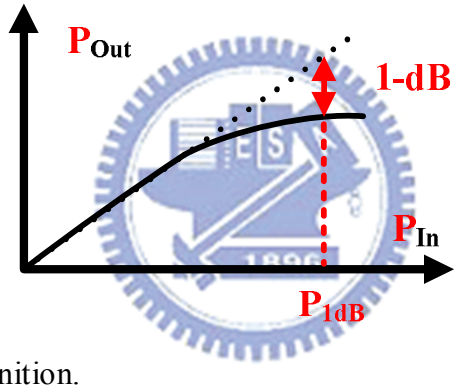

Figure 3 - 3 P_{1dB} definition.

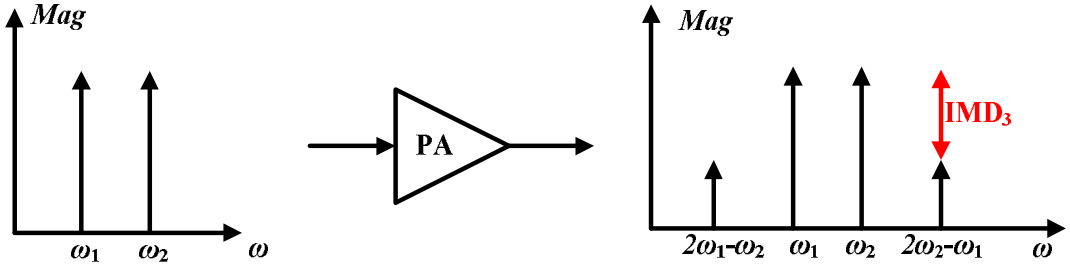

Figure 3 - 4 IMD_3 definition.

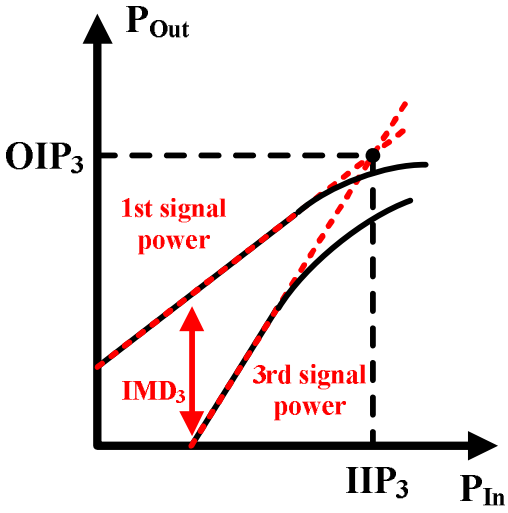

Figure 3 - 5 IIP_3 and OIP_3 definition.

3.1.2 SINGLE-TONE AND TWO-TONE MEASUREMENT

The single-tone measurement is the most essential method to estimate the characteristics of the power amplifier. The frequency response of the nonlinear static and nonlinear dynamic power amplifiers are shown in Figure 3-6 and 3-7.

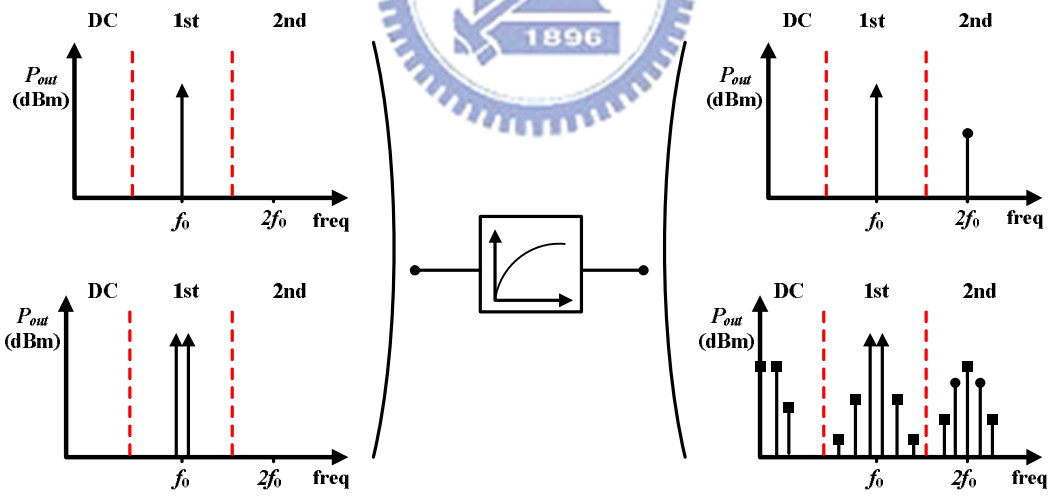

Figure 3 - 6 Responses of a nonlinear static amplifier to a single-tone and a two tone input signal.

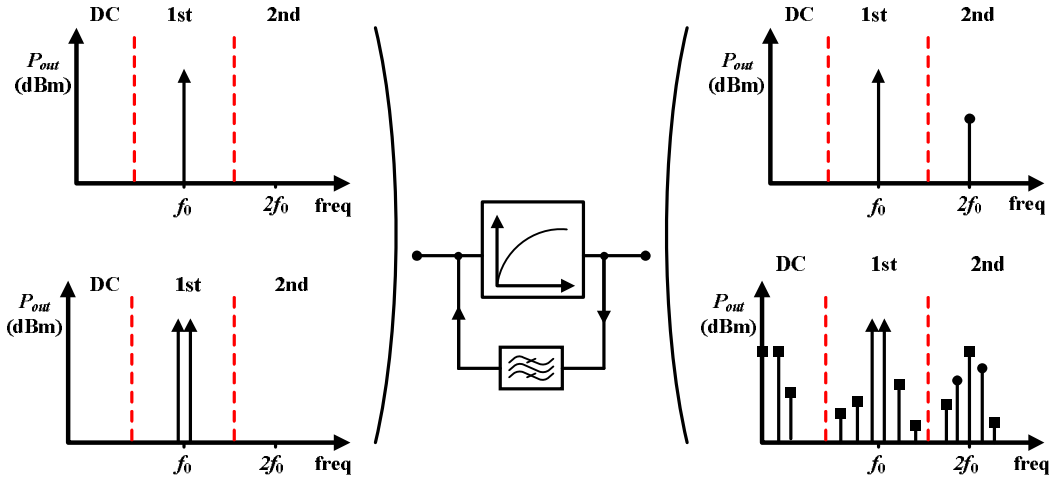

Figure 3 - 7 Responses of a dynamic nonlinear amplifier to a single-tone and a two tone input signal.

The distortion in Figure 3-5 and 3-6 would be considered, especially that are located in the DC, fundamental and second-order harmonic band. However, the two-tone input signal could express the system that is nonlinear static or nonlinear dynamic. The imbalances could be found in two-tone or broadband signal. The additional distortions are generated by adding and subtracting the frequency of the input (ex: f_2-f_1, f_2+f_1, $2f_2$-f_1, $2f_1$-f_2, …). The imbalances in the distortions are generated by nonlinear memory effects. The follows are the tests about a typical Class-AB amplifier. The AM-AM and AM-PM conversions with single-tone measurement are shown in Figure 3-8 and Figure 3-9.

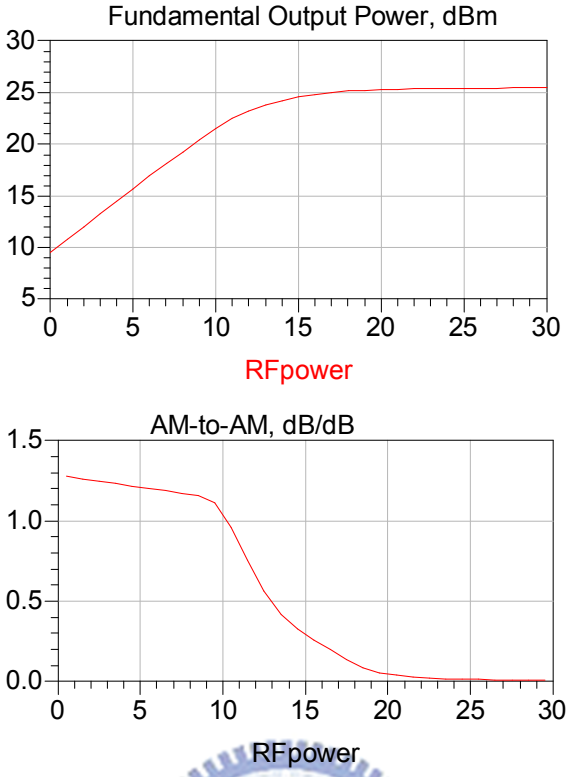

Figure 3 - 8 The AM-AM conversion of a single-tone test.

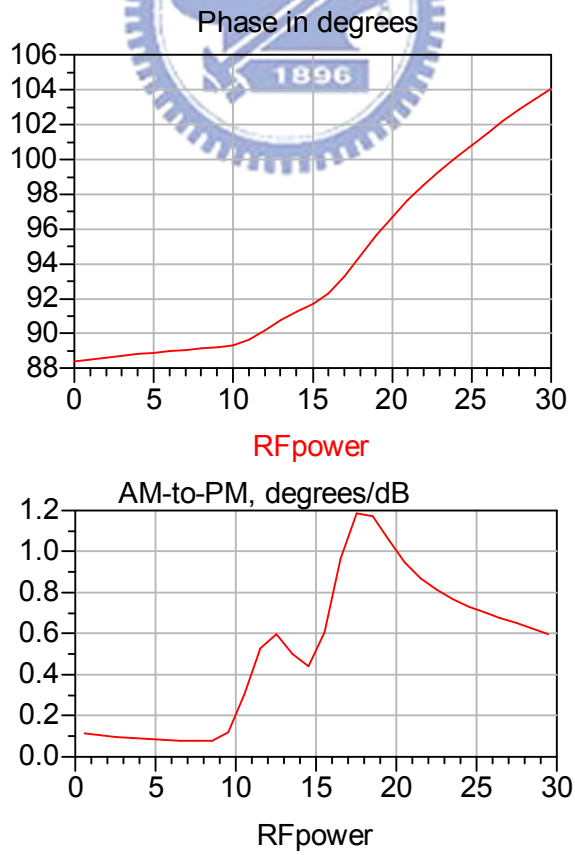

Figure 3 - 9 The AM-PM conversion of a single-tone test.

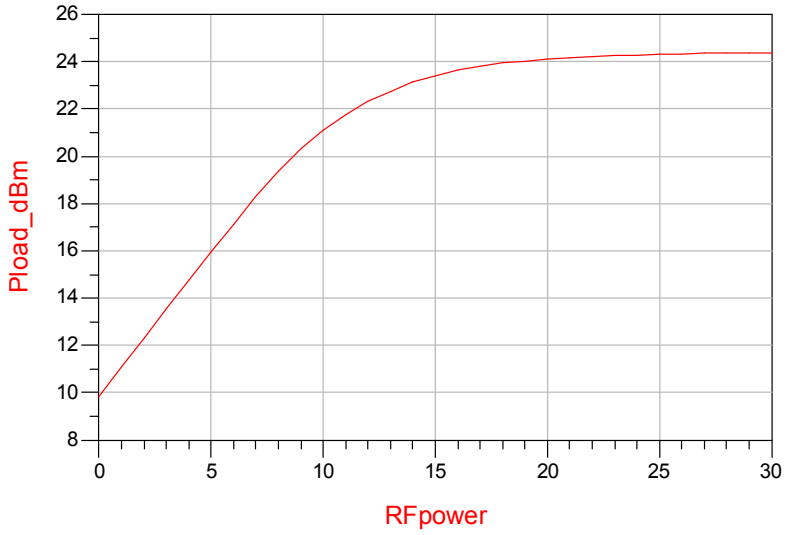

Figure 3 - 10 The output power to input power of a two-tone test.

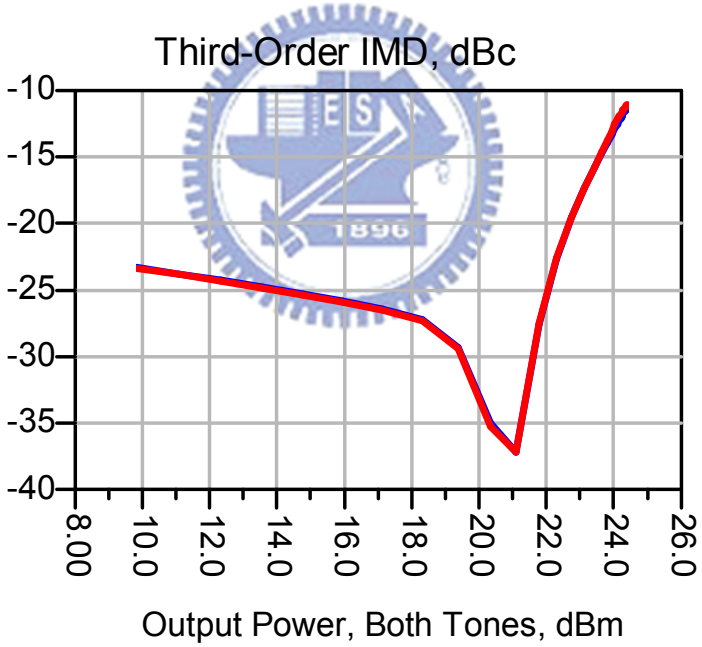

Figure 3 - 11 IMD_3 for different output powers.

By two-tone input signal, the AM-AM conversions are shown in Figure 3-10. The single-tone and two-tone measurement are the general tests for the power amplifiers. These testing have the short simulation time but still have enough information of the power amplifiers modeling. However, the system is getting more

and more complex so the next section will discuss the multi-carrier testing signals.

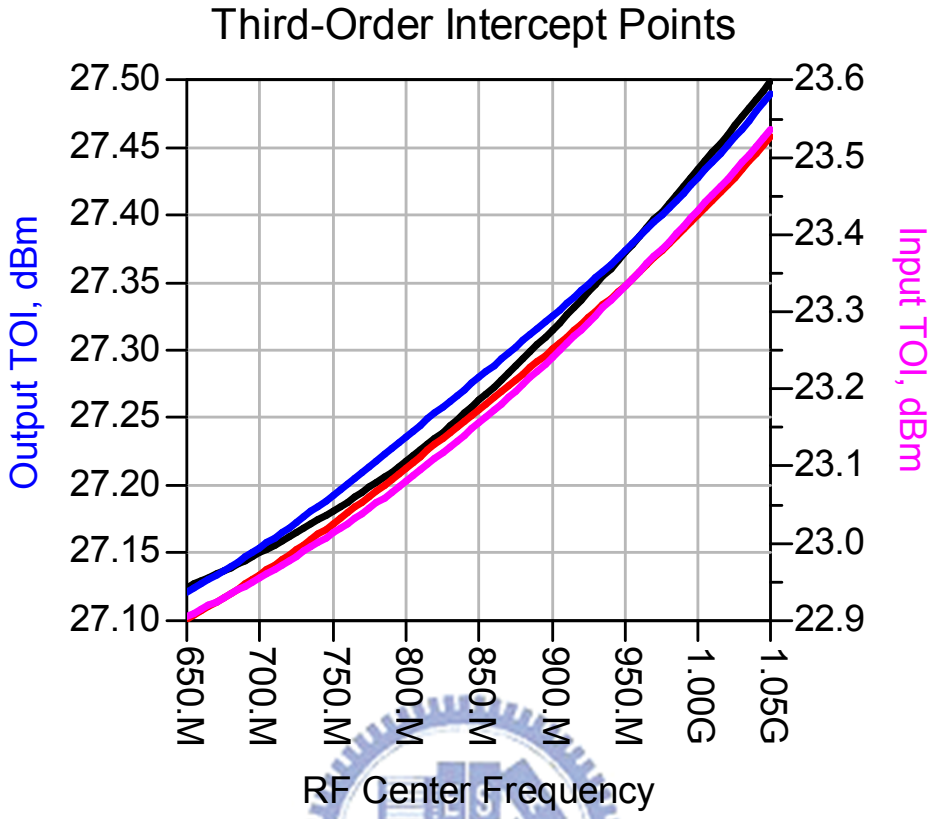

Figure 3 - 12 IP_3 for different frequencies.

3.2 MULTI-CARRIER MEASUREMENT

3.2.1 OVERVIEW OF THE OFDM TECHNOLOGY

At first, this section will introduce the Orthogonal Frequency Division Multiplexing (OFDM) technology. The OFDM system has developed into a popular scheme for wideband digital communications, such as digital television and audio broadcasting, wireless networking and broadband internet access. OFDM is a modulation technology or a multiplex technology. OFDM also could be viewed as be modified from Frequency Division Multiplexing (FDM) technology. The FDM technology is one type of signal multiplexing, and it uses the non-overlapping frequency ranges to transmit different signals. The OFDM signal could earn more spectrum efficiency by spacing the channels closely, as shown in Figure 3-13. The orthogonal carriers would have a narrowband bandwidth. Thus, the symbol rate in the OFDM signal is slow. This technique transforms a frequency-selective wide-band channel into a group of non-selective narrowband channels. The typical OFDM

systems are shown in Figure 3-13 and Figure 3-14.

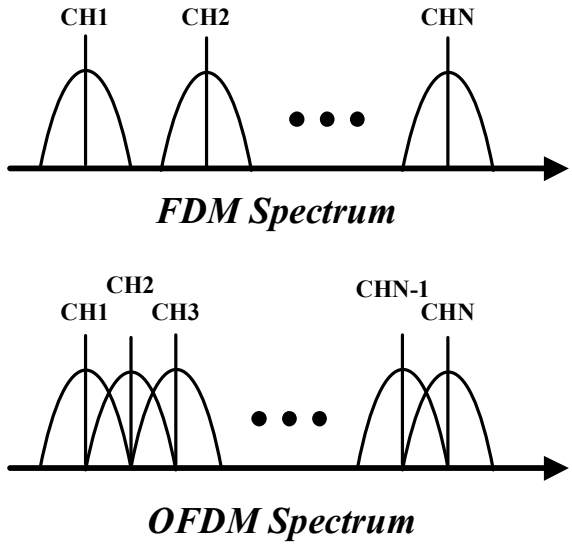

Figure 3 - 13 The typical FDM and OFDM spectrum.

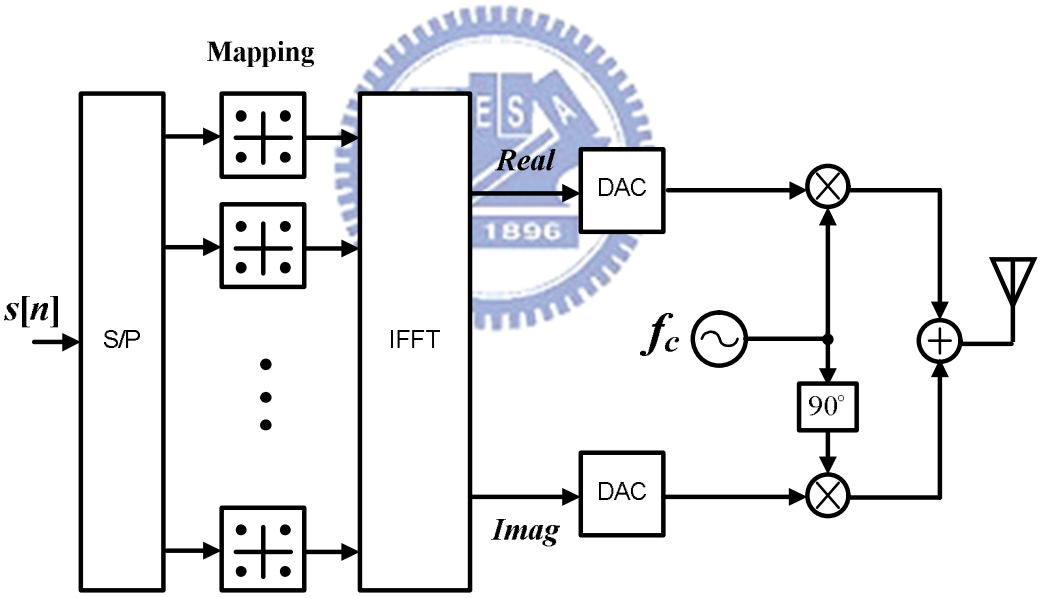

Figure 3 - 14 The typical OFDM system transmitter.

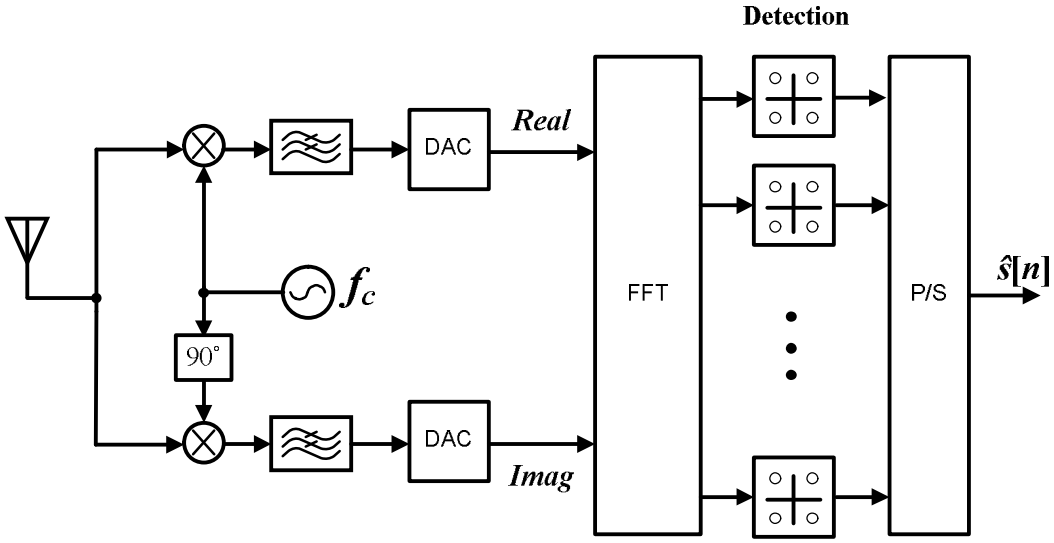

Figure 3 - 15 The typical OFDM system receiver.

Because the OFDM systems are used in wireless communication, the multi-path interference problem should be consider in the signal design. In order to avoid intersymbol interference (ISI) effects from the multi-path, the guard interval (GI) will be added in front of each OFDM symbol. The GIs didn't carry data and are all zero (zero padding). However, the GIs affect the orthogonality of the OFDM signal and causes another problem, namely, the inter-carrier interference (ICI). The symbol cyclic prefix (CP) is a popular method to avoid ISI and ICI effects. The CPs copies partial data of the original OFDM signal, so the new OFDM symbol could keep orthogonal in each symbol.

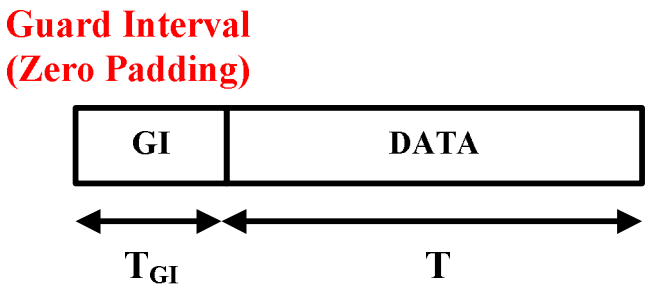

Figure 3 - 16 Guard interval (GI).

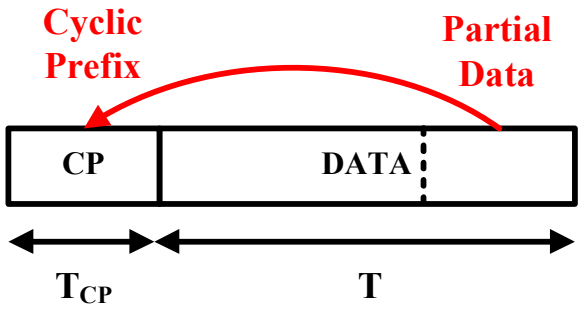

Figure 3 - 17 Cyclic Prefix (CP).

3.2.2 OFDM SIGNAL TESTING

The complex multi-carrier signal with N tones could be expressed as

$$x(t) = \sum_{n=1}^{N} A_n e^{j\left[2\pi(f_0 + n\Delta f)t + \Phi_n\right]}, \tag{3.1}$$

where A_n and Φ_n are the amplitude and phase expression of the n-tone. Then, we should have some new standards to define output measurement. Besides of IIP_n and IMD_n, the Error Vector Magnitude (EVM) is also a standard to quantify the performance of the power amplifiers. What is the EVM [14]? The definition is shown in Figure 3-18, and the input signal is the digital modulated signal. Due to some reasons, such as nonlinearity, noise, outside interference, or imbalance of phase, etc, the output signal vector does not match the reference vector, a product of the input signal and gain. The error vector ê is defined in Equation 3.2.

$$\hat{e} = \left|\vec{M} - \vec{R}\right| \tag{3.2}$$

$$EVM_{rms} = \frac{\sqrt{\frac{1}{N}\sum_{n=1}^{N}\hat{e}^2}}{\sqrt{\frac{1}{N}\sum_{n=1}^{N}\left|\vec{R}\right|^2}} \tag{3.3}$$

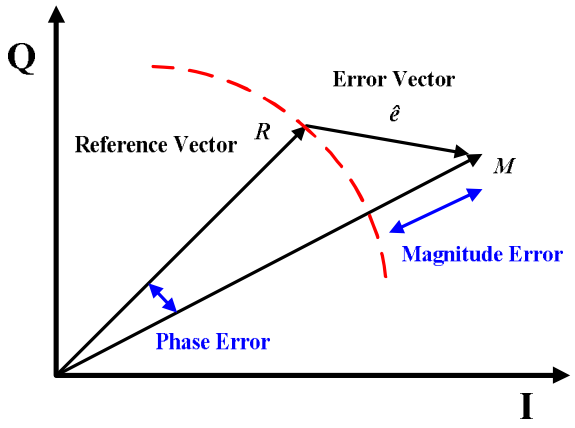

Figure 3 - 18 Error Vector Magnitude (EVM) definition.

3.2.3 REFERENCE OFDM SIGNAL

The reference model in Figure 3-19 is an OFDM signal with QPSK that is made by Muhammad Nadeem Khan in the MATLAB central. This type of OFDM is particularly useful for WiMAX and other Wireless and Multimedia Standards. We revise this OFDM model to fulfill our requirements, and the output spectrum is shown in Figure 3-13. In the Chapter 4, the reference OFDM signal will be used.

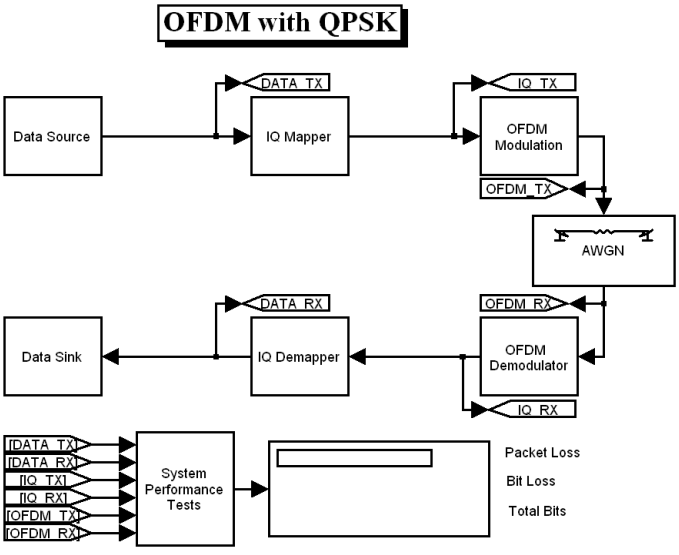

Figure 3 - 19 OFDM with QPSK model by Muhammad Nadeem Khan.

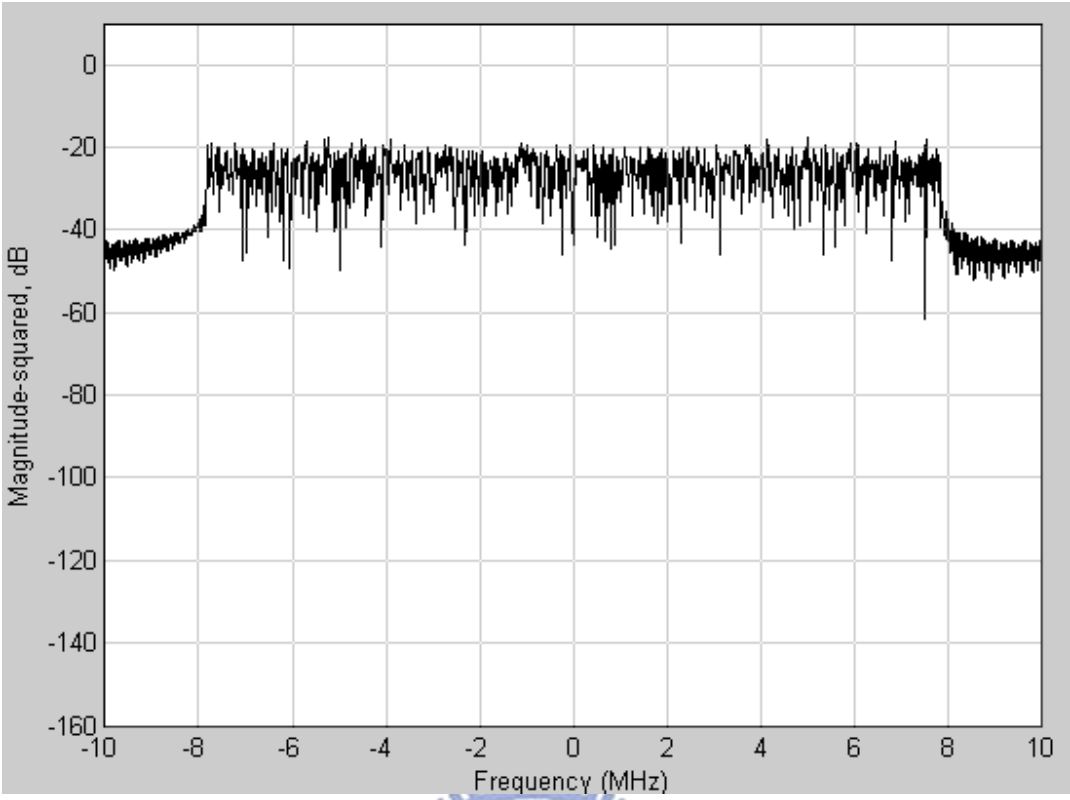

Figure 3 - 20 QPSK OFDM spectrums.

3.3 OFDM SIGNALS WITH GAUSSIAN PDF

3.3.1 ISSUE

Usually the OFDM testing signals are designed by a pseudo-random generator. Therefore, the input signal is a concatenation of several pseudo-random OFDM symbols (frames). The output measurements have to be averaged to obtain the EVM. Adding more frames or more carriers can get higher accuracy. However, a lot of frames will result in long simulation time, and a lot of carriers will result in a complex system. In fact, the accuracy and complexity is a trade-off pair. In this thesis, the designed signal follows the reference model to decide the number of the carriers. The desired signal is an OFDM-modulated signal with its amplitude follows a Gaussian probability distribution functions (PDF) [15, 16]. By the central limit theorem, the summation of a sufficiently large number of independent random variables, each with finite mean and variance, will be approximately normally distributed. The amplitudes in the time domain could be seen as the summation of such independent random

variables. Then, if the designed input signal is an OFDM with the Gaussian PDF for its amplitude, perhaps a short segment of designed input signal can generate an output signal with similar statistics as the output generated by a long segment of pseudo-random OFDM signal.

3.3.2 METHOD

Step 1. Set the ideal spectrum model $S(f)$ in frequency domain and ideal waveform model $w(i)$ in timr domain. These models must have the same power as of the pseudo-random OFDM signals. The waveform model $w(i)$ is made from a Gaussian PDF, and the variable i is the time index of the waveform. In mathematic, it could be written as

$$G(a) = \frac{1}{\sigma\sqrt{2\pi}} e^{-\frac{(a-\mu)^2}{2\sigma^2}}, \tag{3.4}$$

where the function $G(a)$ is a Gaussian PDF and the parameter a is the amplitude. Here, define the mean μ = 0 and the variance is σ. Then, assume the function $N(a)$ is the number of each amplitude value ai and the variable n is the number of the carrier. The Equation could be changed to

$$N(a) = n \cdot G(a) = n \cdot \frac{1}{\sigma\sqrt{2\pi}} e^{-\frac{a^2}{2\sigma^2}}. \tag{3.5}$$

Define the sum of OFDM signal power is the constant P, and we can get the Equation (3.6).

$$\begin{aligned} P &\approx \int_{-\infty}^{\infty} a^2 \cdot N(a) da \\ &= \int_{-\infty}^{\infty} a^2 \cdot \frac{n}{\sigma\sqrt{2\pi}} e^{-\frac{a^2}{2\sigma^2}} da \\ &= \frac{n}{\sigma\sqrt{2\pi}} \cdot \int_{-\infty}^{\infty} a^2 e^{-\frac{a^2}{2\sigma^2}} da \\ &= \frac{n}{\sigma\sqrt{2\pi}} \cdot \left[\frac{1}{2} \cdot \sqrt{\pi (2\sigma)^3} \right] = n \cdot \sqrt{\sigma} \end{aligned} \tag{3.6}$$

Then, the adequate variance σ could be found, and the function $w(i)$ could be designed. The spectrum function $S(f)$ had the same bandwidth with the standard model.

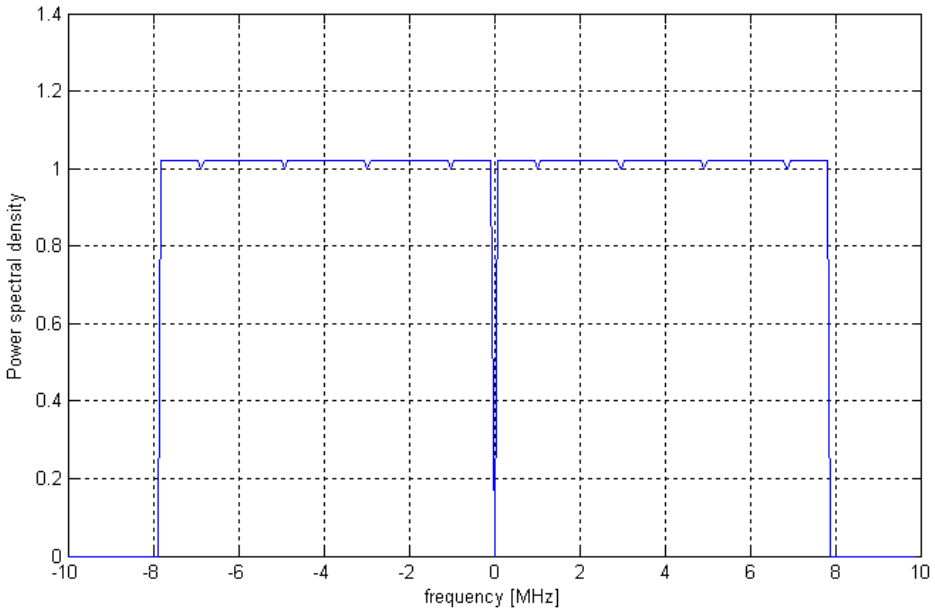

Figure 3 - 21 Ideal spectrum function $S(f)$.

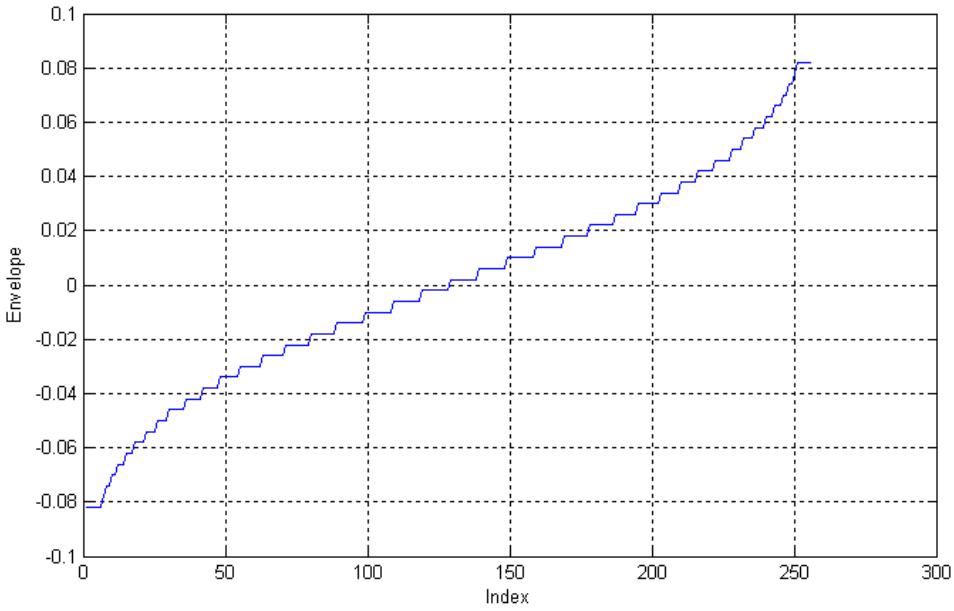

Figure 3 - 22 Ideal waveform function $w(i)$.

Step 2. Generate an original signal $x(t)$. The designed signal will have little discrepancy between different original signals.

Step 3. Use the fast Fourier transform (FFT) to convert the original signal $x(t)$ to the spectrum $X(f)$ in the Figure.

$$x(t) \xrightarrow{FFT} X(f) \tag{3.7}$$

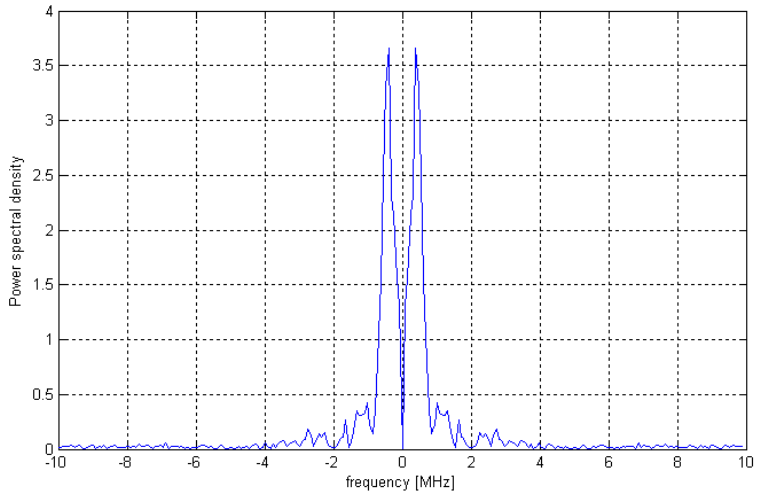

Figure 3 - 23 Original spectrum $X(f)$.

Step 4. Replace the magnitude spectrum by the ideal model $S(f)$, combined with the original phase spectrum. This is redefined as the modified spectrum $\hat{U}(f)$.

$$\hat{U}(f) = |S(f)| \cdot e^{j(\angle X(f))} \tag{3.8}$$

Step 5. Use the inverse fast Fourier transform (IFFT) to convert the modified spectrum $\hat{U}(f)$ in Step 4 to the time signal $\hat{u}(t)$ in the Figure 3-24.

$$\hat{U}(f) \xrightarrow{IFFT} \hat{u}(t) \tag{3.9}$$

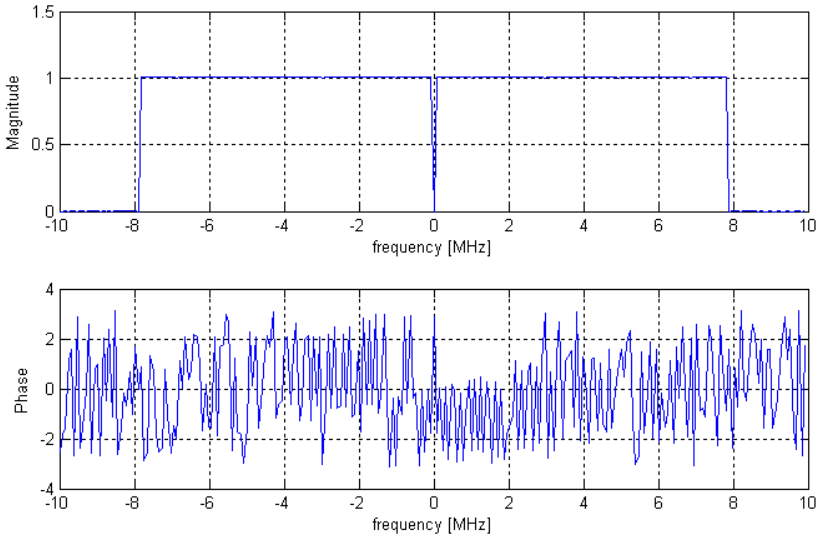

Figure 3 - 24 The modified spectrum $\hat{U}(f)$ and time signal $\hat{u}(t)$ in first cycle.

Step 6. According the gradation of the envelope, replace the magnitude of the signal $\hat{u}(t)$ by ideal waveform model $w(i)$. The new signal in time domain is called as $\hat{o}(t)$ that is shown in Figure 3-25.

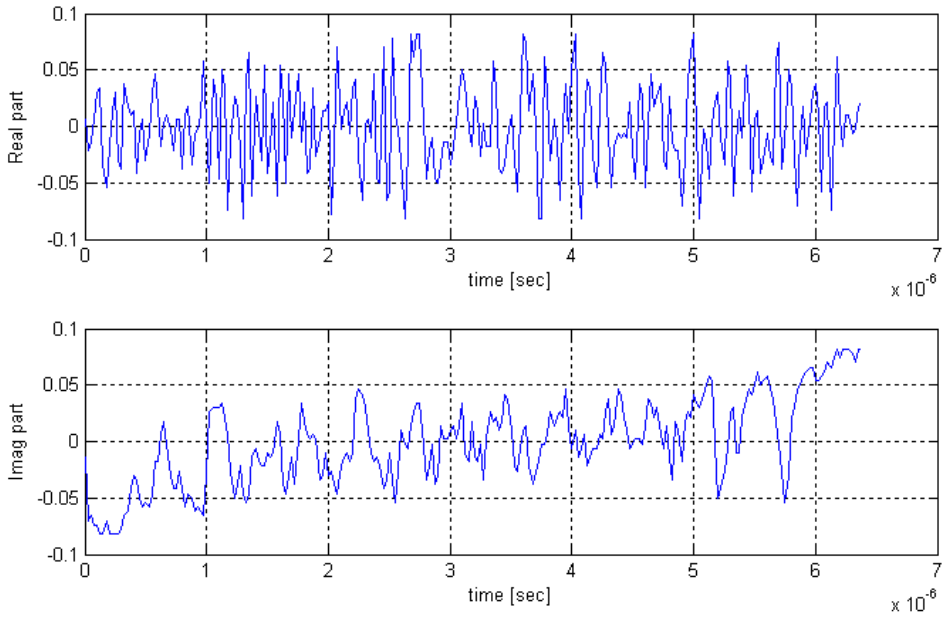

Figure 3 - 25 The modified time signal $\hat{o}(t)$ in first cycle.

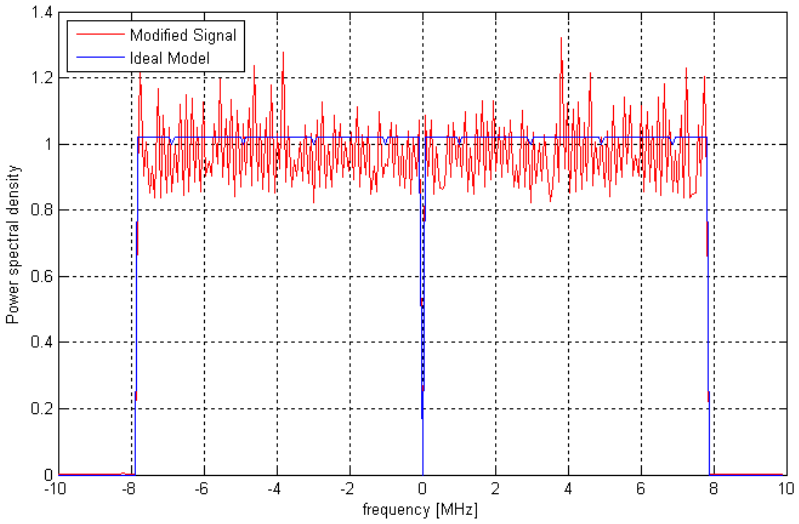

Figure 3 - 26 Spectrum $S(f)$ and $\hat{O}(f)$ didn't match.

Step 7. Use the FFT to convert the signal $\hat{o}(t)$ to the spectrum $\hat{O}(f)$. Then, we could find that the spectrum might not match the ideal model $S(f)$ in Figure 3-20. The designed signal $\hat{O}(f)$ is hard to satisfy the ideal model $S(f)$ and $w(i)$ at the same time. For this reason, we have to repeat the process from Step 3 to Step 7. The modified signal will converge after several cycles. The converged baseband signal $\hat{g}(t)$ is shown in Figure 3-27.

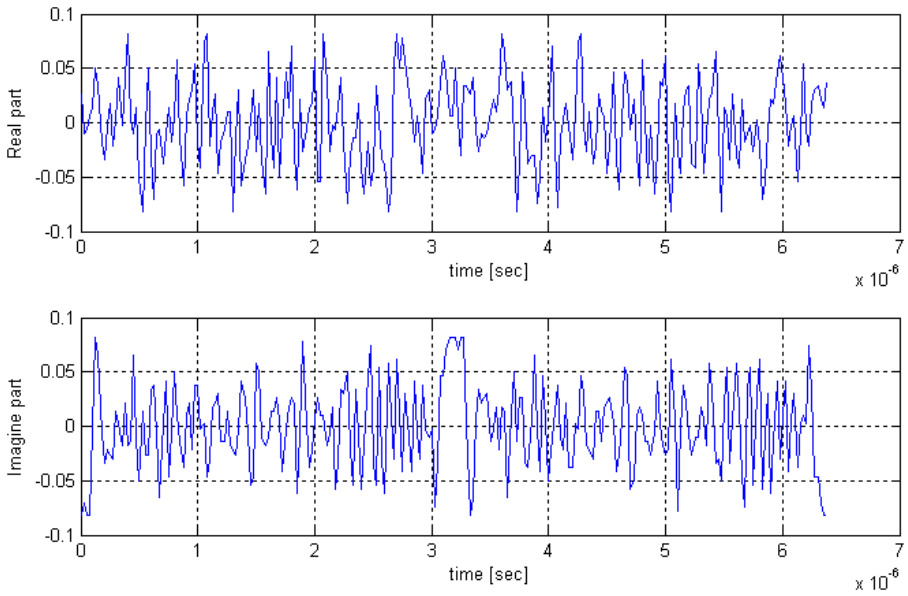

Figure 3 - 27 Time domain signal $\hat{g}(t)$.

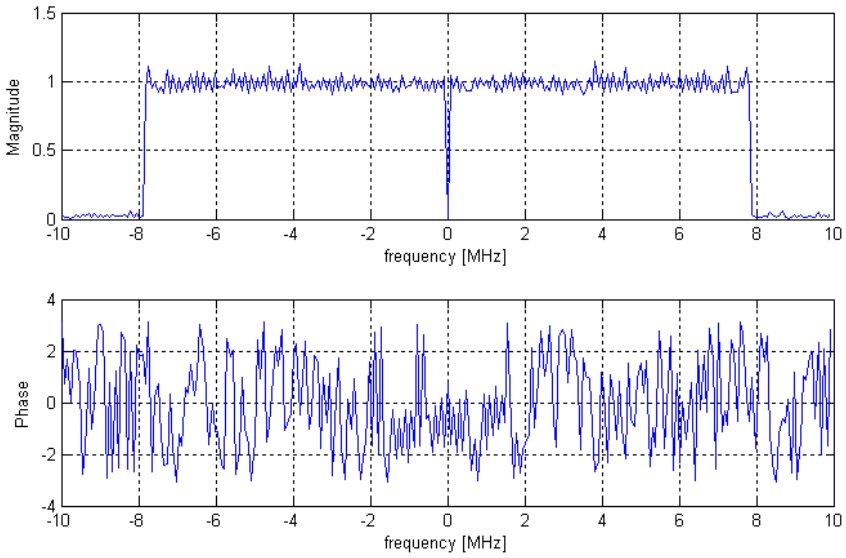

Figure 3 - 28 Spectrum $\hat{G}(f)$.

Step 8. From Step1 to Step7, we designed a baseband signal $\hat{g}(t)$ with the same bandwidth, and its envelope is a Gaussian PDF. Then, modulate the signal $\hat{g}(t)$ to the passband frequency. At first, the signal $\hat{g}(t)$ is be upsampled. The upsampling spectrum $G(f)$ is shown in Figure 3-29.

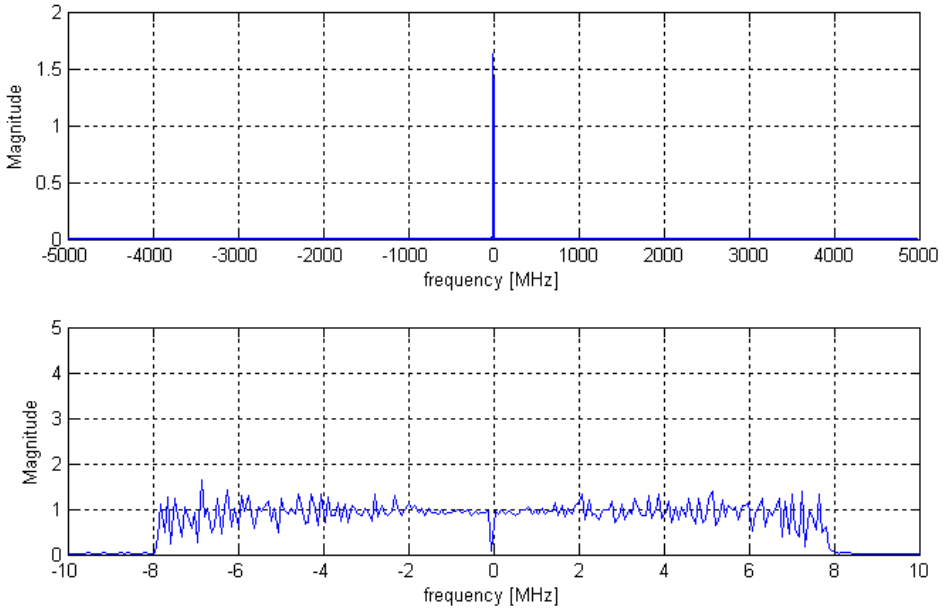

Figure 3 - 29 Spectrum $G(f)$ with upsampling.

Step 9. From Equation, the baseband signal ĝ(t) is modulated to high frequency

band. The final y(t) and its spectrum Y(f) will be shown in Figure 3-30 and 3-31.

$$FFT\ pairs \begin{Bmatrix} Y(f) = \hat{G}(f \pm f_c) \\ y(t) = \hat{g}(t) \cdot e^{\pm j2\pi f_c t} \end{Bmatrix} \tag{3.10}$$

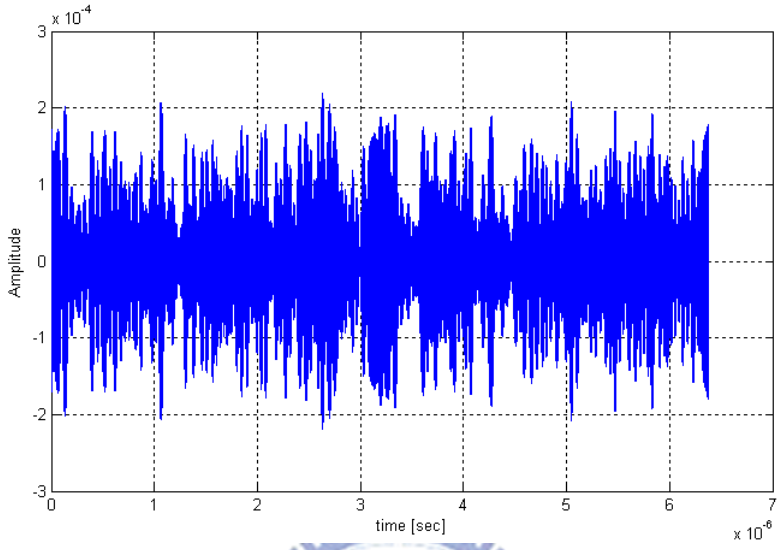

Figure 3 - 30 The passband time signal $y(t)$.

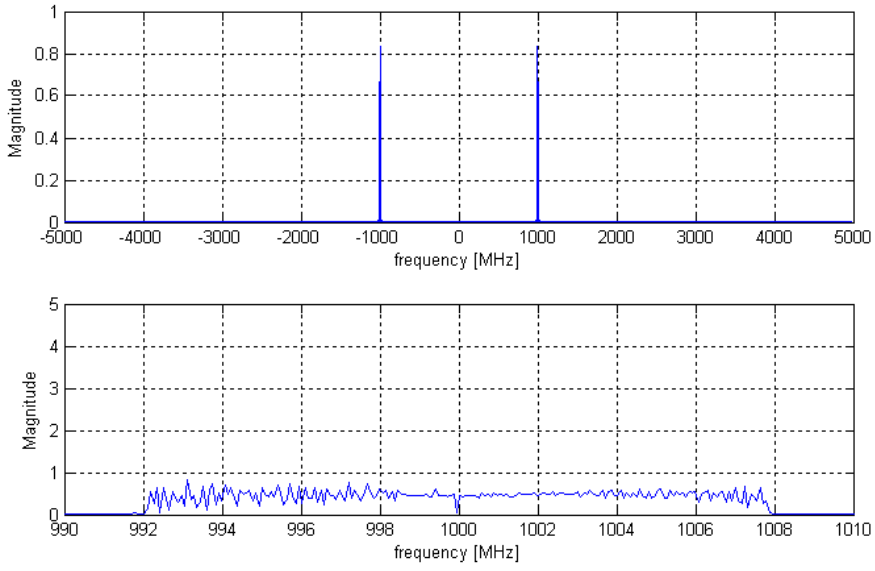

Figure 3 - 31 The passband spectrum $Y(f)$.

Now, the OFDM signal with a Gaussian PDF envelope has already made. The next section will describe how to do simulations with this signal.

3.4 CO-SIMULATION

In the previous section, we have made the OFDM signal with the Gaussian PDF envelope. Now, this section will discuss how to simulate PAs' behavior with this signal. There are many software packages for designing circuit. The Advance Design System (ADS) is a good tool of RF simulation needs. It has two types of schematics, analog (RF) or digital. In general, the engineers usually use the analog interface to design a power amplifier. Unfortunately, if the input signals for simulation are multi-carrier or some complex signals, simulations will need a lot of time and more complex setup. In order to simulate PA with OFDM signals, we decide to do the co-simulation in the ADS. The structure is shown in Figure 3-32.

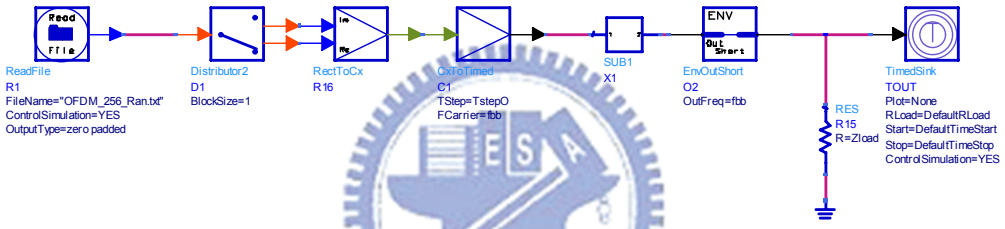

Figure 3 - 32 ADS environment.

The DUT is set in the subsystem, and the input signal will be read by from a file. The ADS has some communication blocks to modulate the signal, and it's a way to design the passband signal. In the co-simulation, the analog box can just choose the envelope or transient simulation, and the envelope simulation is faster. I designe the input signal by MATLAB and simulate the whole PA by ADS. In order to compare between the designed signal with a Gaussian PDF envelope and the pseudo-random OFDM signal, the environment will keep the same. Some parameters will use default value by ADS setting. The output signal is converted by ADS function shown in Figure 2-33.

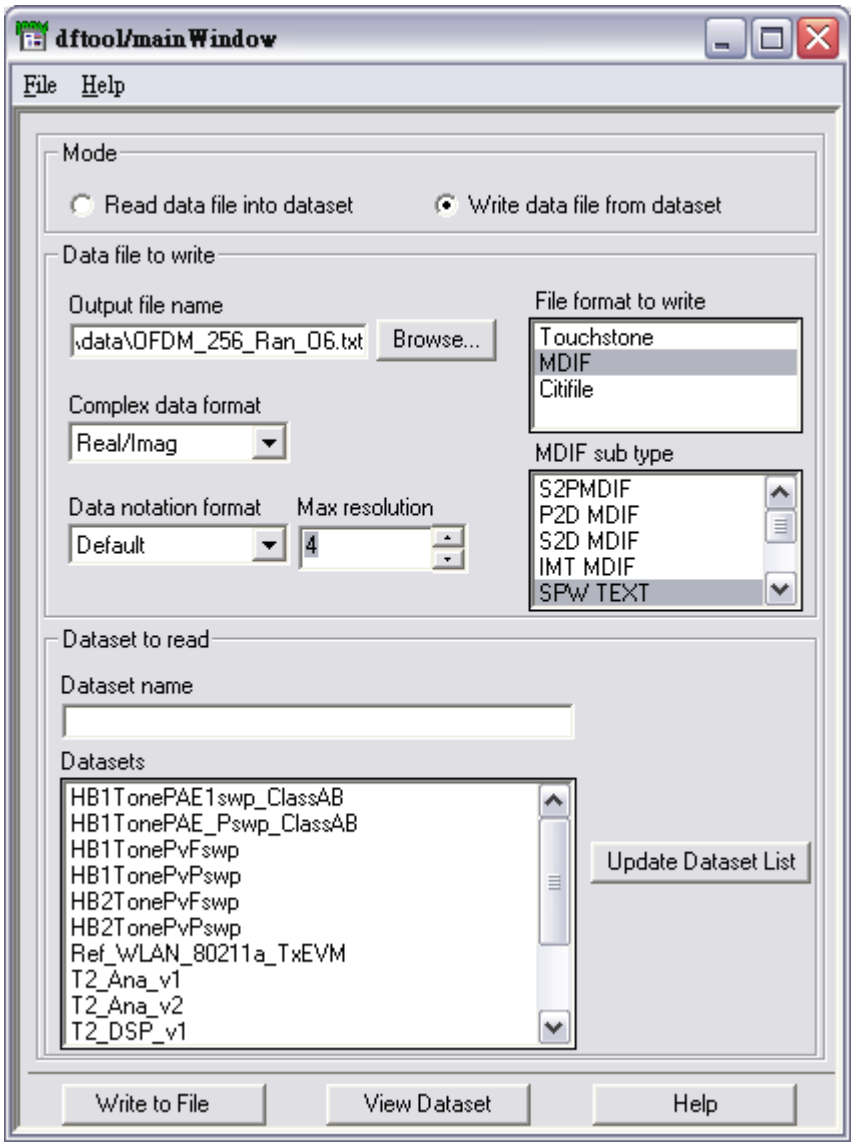

Figure 3 - 33 Data File Tool in ADS system.

The output file is in .TXT format and will be read back to MATLAB in which EVM and some results can be calculated. Thus, the output spectrum could be observed by ADS and processed in MATLAB. The result will be shown in Chapter 4.

Chapter 4
Results and Conclusions

4.1 RESULT

4.1.1 RESULT OF THE QPSK OFDM SIGNAL

The pseudo-random QPSK OFDM signals are generated by the reference MATLAB model. The input data file is read with text format and simulated by ADS. In order to reduce simulation time, the QPSK signal is divided into several parts. The output signals in time domain would be combined and processed by MATLAB. We transfer the data to the first quadrant and calculate the result. The output data has phase shifts, and we correct the effects before calculating EVM. The EVM of the QPSK OFDM signal are defined in Chapter 3 and shown in Figure 4-4. The EVM in the guard band are meaningless because input signals should be all zeros in that band. Therefore, we will define them as zero. In Figure 4-4, the reference vectors are calculated by each point. In Figure 4-5, the new reference vector will be defined with same magnitude, and the EVM value will be changed. The result in Figure 4-4 is worse than the result in Figure 4-5.

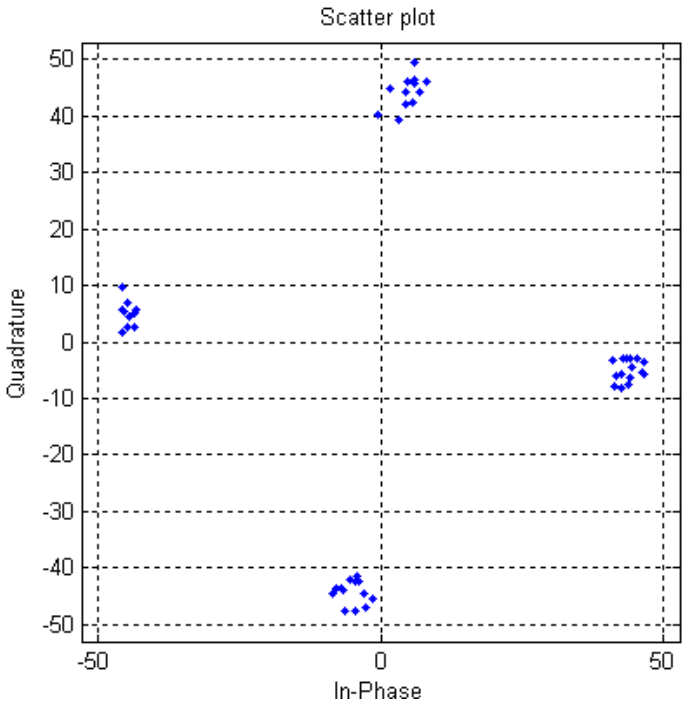

Figure 4 - 1 Original output data in scatter plot.

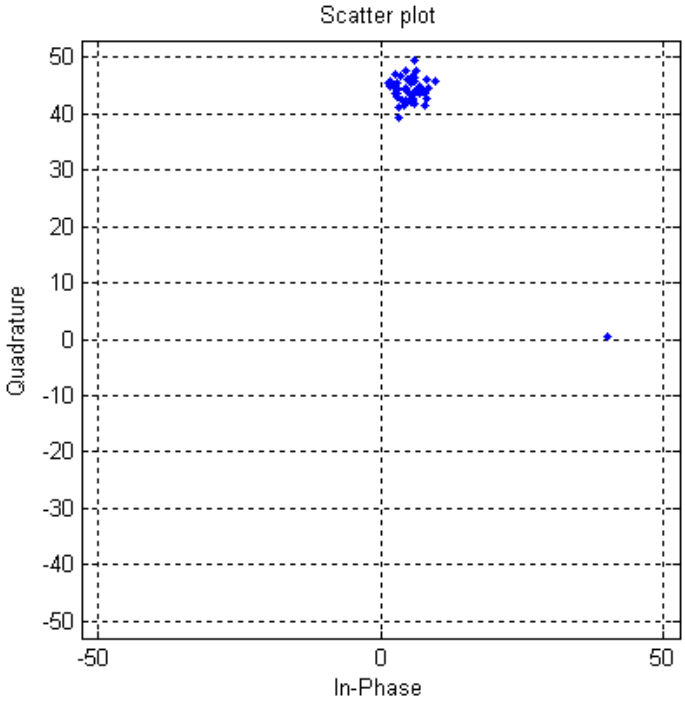

Figure 4 - 2 Transfer data to first quadrant with wrong method.

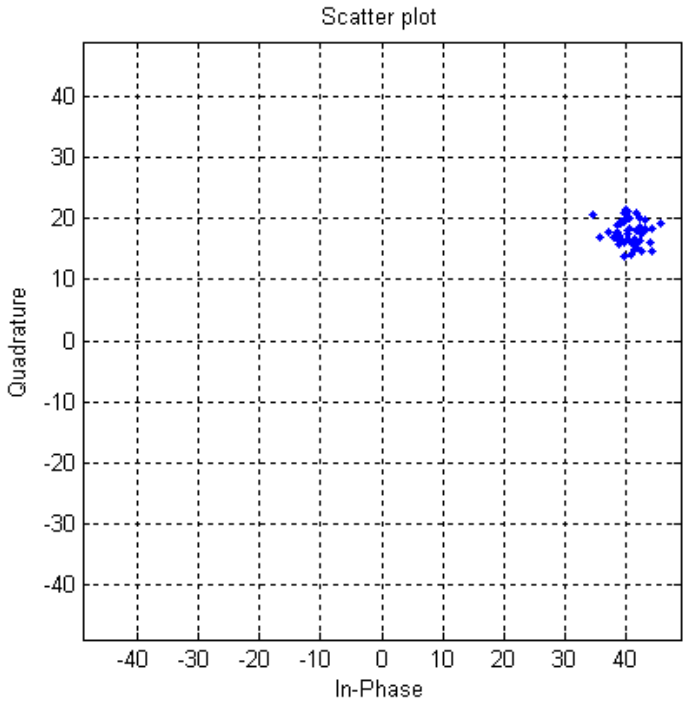

Figure 4 - 3 Transfer data to first quadrant with correct method.

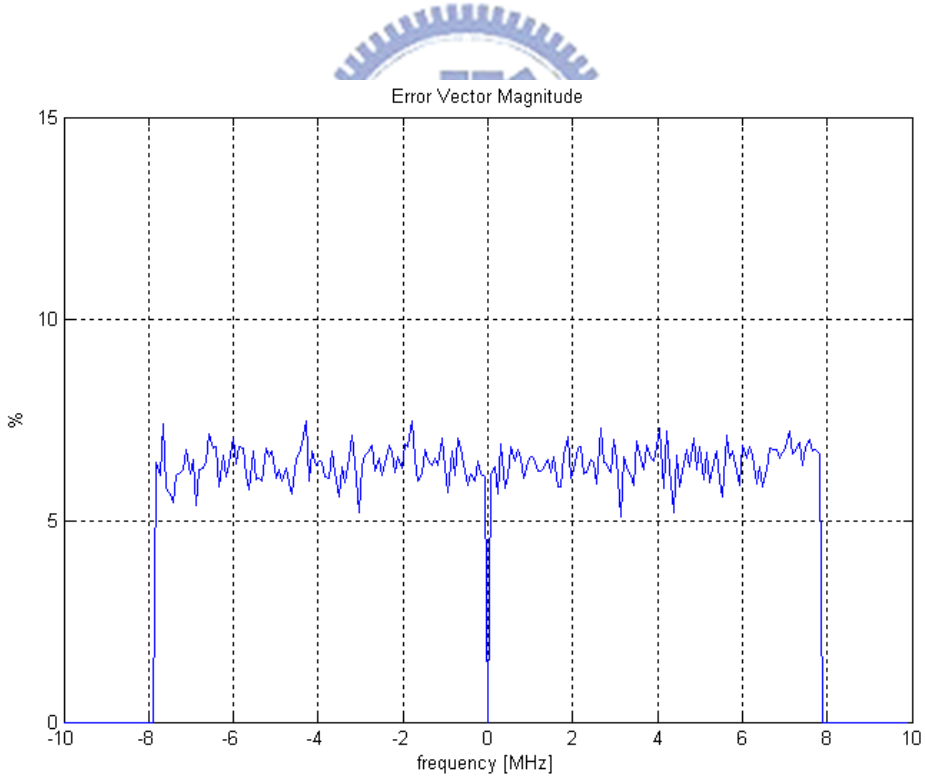

Figure 4 - 4 Error vector magnitude of the QPSK signal.

$$EVM_{rms} = 6.427\%$$

$$EVM_{\text{var}} = 2.679\%$$

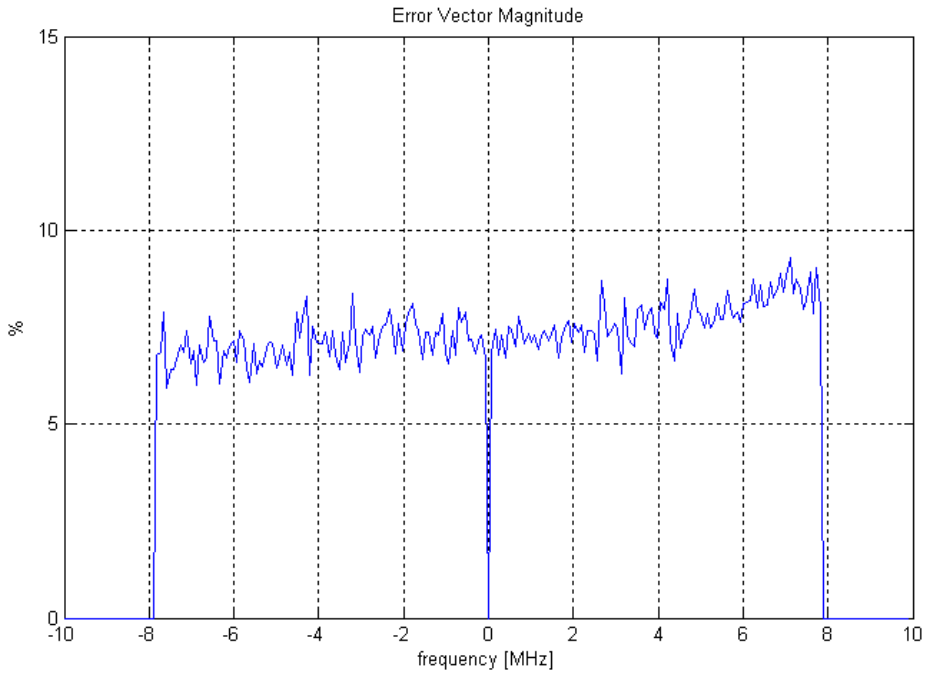

Figure 4 - 5 Error vector magnitude of the QPSK signal with same standard.

$$EVM_{rms} = 7.422\%$$

$$EVM_{\text{var}} = 3.110\%$$

4.1.2 OFDM SIGNAL WITH GAUSSIAN PDF ENVELOPE

Simulations with the designed signal will be conducted in the same way. Of course, the EVM in the guard band will be also defined as zero. The output signal SO and input signal SI are shown in Figure 4-6. We would calibrate the output signal in Equation 4.1 and calculate EVM in Figure 4-8. We also designed a double length signal in Figure 4-9.

$$X_{Output}(t) = Gain_{opi} \cdot X_{Input}(t-\tau) \tag{4.1}$$

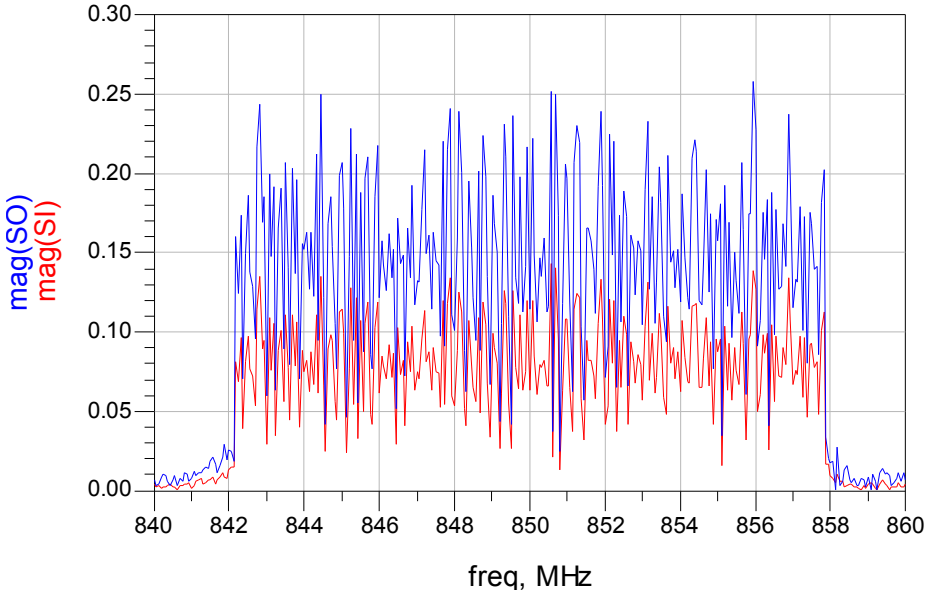

Figure 4 - 6 Spectrums of the output (SO) and input (SI) signals with ADS.

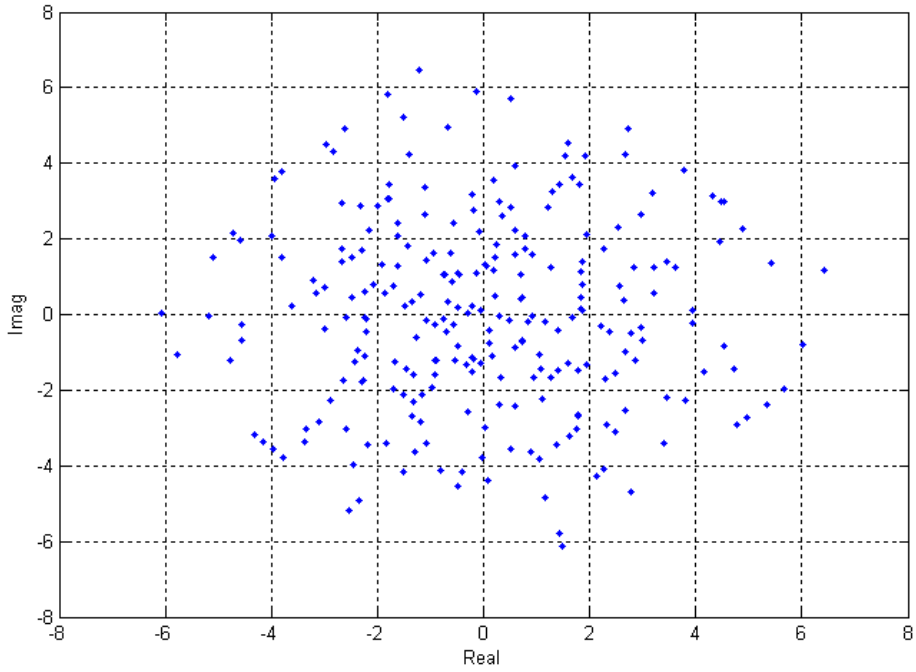

Figure 4 - 7 Real part and imagine part of the EVM.

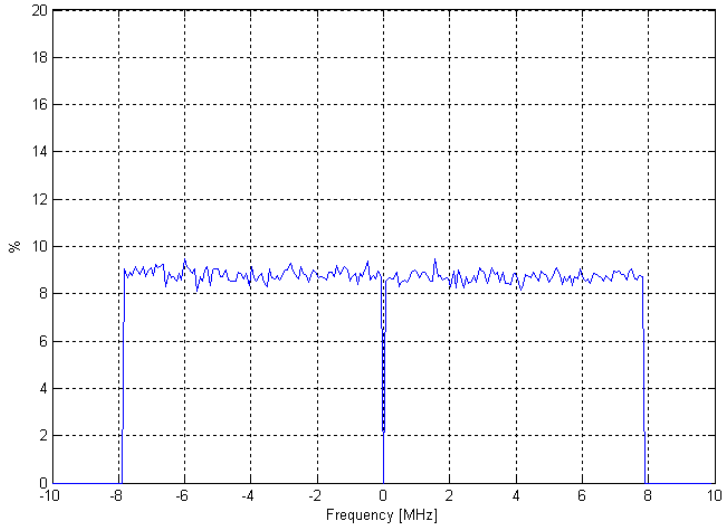

Figure 4 - 8 Error vector magnitude of the designed signal.

$$EVM_{rms} = 8.770\%$$

$$EVM_{\text{var}} = 3.631\%$$

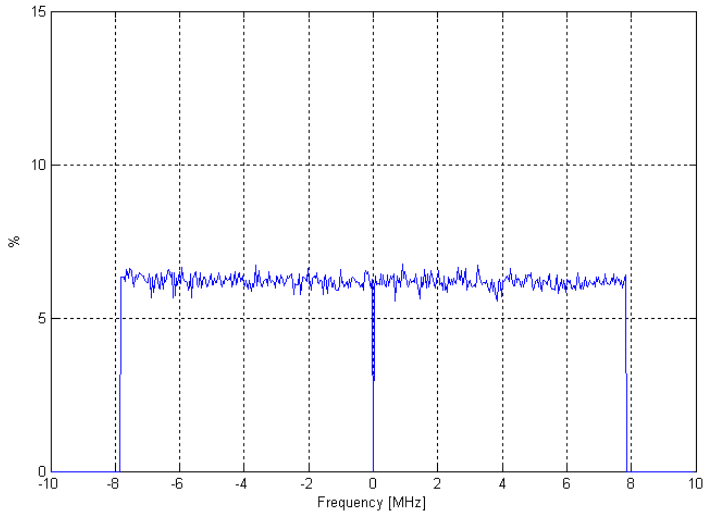

Figure 4 - 9 Error vector magnitude of the designed signal with double length.

$$EVM_{rms} = 6.190\%$$

$$EVM_{\text{var}} = 2.565\%$$

4.2 CONCLUSION

In past, the error vector magnitude is measured by the long-term averaging of error vectors associated with the pseudo-random OFDM signal. The simulation would take a lot of time. I hope to develop a simulation method with a specially designed signal such that the simulation time can be cut drastically. To this end, partial success is obtained. The EVM of the designed signal is higher than the EVM of the random OFDM signal, and the graphs are not the same completely. However, if the length of the design signal is increased, a much better result of EVM can be obtained. Another way to calculate EVM of pseudo-random OFDM signals is to fix a constant gain factor for all sub-carriers, and the deviation of gains among sub-carriers would be counted into EVM. The EVM thus obtained would also increase and get closer to the EVM value obtained with the designed signal. It is not clear yet which procedure should be adopted as the standard method to calculate EVMs and to compare the results obtained from pseudo-random OFDM signals and our designed signals. These topics are worth further investigation and should be considered as future works. There are also some other problems in this test. At first, the OFDM signal usually has phase-shift effect. Then, I did not cancel the phase-shift well. In the random QPSK OFDM signal process, the EVM calculations are based on the root-mean-square value of the output result. Therefore, the random signal could have less phase-shift effect and get good reference vector. On the hand, the original signal before the design would affect the output design signal. With more controlled design conditions, we might have some better choices to design and the original signal effect could decrease. We could also try to increase length of design signals, and we could see the better results. The next topic is how to decide the better standard that could calculate fairly EVM between reference signals and designed signals. Then, we could decide the length of designed signal and the measurement method of reference signals. Nevertheless, the designed OFDM signal with Gaussian PDF could be used to measure the power amplifiers much more quickly.

4.3 FUTURE WORKS

The problems in the conclusion would need to find some better methods. Because I don't have enough time to study my research, the excitation signal just is one kind of the random QPSK OFDM signal. If the signals are other modulations, the difference between designed signal and random modulated signal could be changed. The relationship is a new topic to research. Then, we add the conditions to design a signal, and the EVM graphs could be closer. The number tones of the signal would affect the exactness that is proved in the reference papers. However, the difference number of the design cycle would affect the shape of the excitation signal. The relationship of the cycle number is also a new question. Now, the systems are more complex so we need more correct models and signals to design.

REFERENCES

[1] D. Schreurs et al., *RF Power Amplifier Behavioral Modeling*, Cambridge University Press, 2009.

[2] T. H. Lee, *The Design of CMOS Radio-Frequency Integrated Circuits*, second edition, Cambridge University Press, 2004.

[3] A. A. M. Saleh, "Frequency-independent and frequency-dependent nonlinear models of TWT amplifiers," *IEEE Trans. Communications*, vol. 29, no. 11, pp.1715-1720, November 1981.

[4] M. S. O'Droma, "Dynamic range and other fundamentals of the complex Bessel function series approximation model for memoryless nonlinear devices," *IEEE Trans. Communications*, vol. 37, no. 4, pp. 397-398, April 1989.

[5] P. Hetrakul and D. P. Taylor, "Nonlinear quadrature model for traveling-wave tube type amplifier," *Electronics Lett.*, vol. 11, p. 50, January 1975.

[6] A. L. Berman and C. H. Mahle, "Nonlinear phase shift in traveling-wave tubes as applied to multiple access communication satellites," *IEEE Trans. Communications*, vol. 18, pp.37-48, February 1970.

[7] M. C. Jeruchim, P. Balaban and K. S. Shanmugan, *Simulation of Communication Systems, Modeling, Methodology and Techniques*, second edition, Kluwer/Plenum, 2000.

[8] A. A. Moulthrop et al., "A dynamic AM/AM and AM/PM measurement technique," *IEEE MTT-S Int. Microwave Symposium Digest*, vol. 3, pp. 1455-1458, June 1997.

[9] R. Blum and M. C. Jeruchim, "Modeling nonlinear amplifiers for communication simulation," in *Proc. IEEE Int. Conf. on Communication*, pp. 1468-1472, June 1989.

[10] C. J. Clark et al., “Power-amplifier characterization using two-tone measurement technique,” in *IEEE Trans. Microwave Theory Tech.*, vol. 50, no. 6, pp. 1590-1602, June 2002.

[11] M. Abuelma’atti, “Frequency-dependent nonlinear quadrature model for TWT amplifiers,” *IEEE Trans. Communications*, vol. 32, no. 8, pp. 982-986, August 1984.

[12] P. Draxler et al., “Time domain characterization of power amplifiers with memory effects,” in *IEEE MTT-S Int. Microwave Symposium Dig*., pp. 803-806, June 2003.

[13] T. Söderström and P. Stoica, *System Identification*, Prentice Hall, 1989.

[14] E. Acar, S. Ozev and K.B. Redmond, “Enhanced Error Vector Magnitude (EVM) Measurements for Testing WLAN Transceivers,” iccad, pp. 210-216, 2006 *IEEE/ACM Int. Conf. on Computer Aided Design*, 2006.

[15] M. Myslinski et al., “A measurement-based multisine design procedure,” in *Proc. Integrated Non-linear Microwave and Millimeter-wave Circuits Workshop*, pp. 52-55, January 2006.

[16] J. P. Pedro and N. B. Carvalho, “Design multi-sine excitations for nonlinear model testing,” IEEE Trans. on Microwave Theory and Tech., vol. 53, no. 1, pp. 45-53, January 2005.